RICE

RICE UNIVERSITY

MECH 407: CAPSTONE DESIGN PROJECT I

SPRING 2025 FINAL REPORT

MAY 6TH 2025

TEAM NAME:

M.U.D.K.I.P

maddo.kippu.3256@gmail.com

TEAM MEMBERS:

Lucas Dovalina

Andrew Dahm

Marvyn Raya

Jesus Guajardo

Bill Nguyen

Bryant Huang

Table of Contents

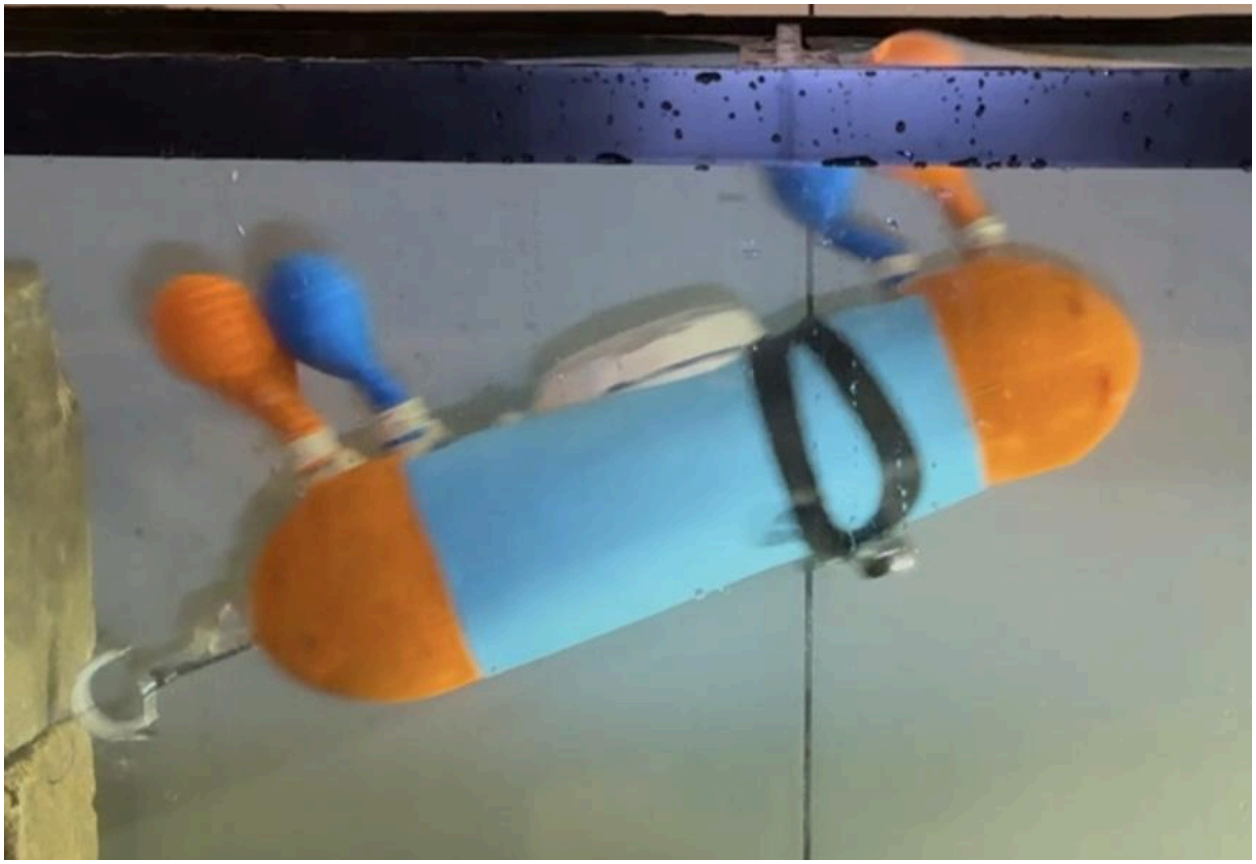

Introduction/Executive Summary

Our senior design project is inspired by the mudskipper, an amphibious fish that can swim in water, move on land, and leap up to two times their length. Mudskippers perform various feats that can be studied and mimicked with advanced technology. By learning how they move—using their fins and tail for propulsion—we sought to design a device that can do the same: swim, jump, and glide when needed. Naturally, our team strived to develop a bioinspired robot that mimics all those attributes. However, given the complexity of those mechanisms and the novelty of researching passive gaseous hydrogen-oxygen-driven dynamics, the team concurred with our advisors that a narrower scope of deliverables was necessary. Thus, we decided to primarily focus on the horizontal propulsion driven by hydrogen-oxygen combustion of the robot inside the water, as well as its ability to rise towards the water's surface with buoyancy control. Additionally, unlike traditional robots, our device will be powered by electrolyzers. Our electrolyzer usage also offers an alternative energy source (compared to conventional energy sources like nuclear, electricity, or diesel) via combustion reaction and means of underwater propulsion, unlike the ubiquitous propeller system. This kind of robot could be helpful in exploring aquatic environments, monitoring ecosystems, or even aiding in rescue missions by utilizing the biomechanics of the mudskipper.

This research is sponsored by Dr. Fathi Ghorbel and Dr. Laura Schaefer of the Robots and Intelligent Systems (RiSYS) and the ESL (Energy Systems) Labs, respectively. There has been a joint research effort between the two on fuel cell robotics, and our project is currently extending this research into the domain of soft robotics.

Prior work

Our predecessors, Team Bay-Max, successfully achieved many of their year-long objectives. They demonstrated several innovative capabilities of Buoyancy Control Devices (BCDs) that had never been implemented on a functioning robot while identifying intriguing design challenges and potential improvements for the existing concept. Notably, they became the first team to showcase BCD control across three degrees of freedom—depth, pitch, and roll. This was done by powering a reversible fuel cell in electrolysis mode to generate H_2 and O_2 gas that filled balloons and increased the robot's buoyancy. Theoretically, they could run the reversible fuel cell as a fuel cell to convert the gas in the balloons to water and electricity, thus reducing the robot's buoyancy to sink. However, this was never demonstrated at a significant scale due to inefficiencies with the reversible fuel cell. One major problem was how water produced during the fuel cell mode would clog up the pipes where the gas should be exiting during electrolysis mode, preventing proper electrolysis function since the gas pressure was not strong enough to push the water out. Team Bay-Max also explored the combustion of gaseous hydrogen-oxygen as a method of propulsion, but found it extremely limiting due to the smaller energy density of the fuel mixture when compared to its liquid propellant counterparts. Despite this immense difference in gravimetric energy density, the combustion of this gaseous fuel can demonstrate utility in specific applications.

Our research advisor, Professor Ghorbel, had a previous collaboration with the University of Houston working on underwater soft robotics as well. UH also demonstrated using reversible fuel cells for buoyancy control with a setup similar to Team Bay-Max. However, one technology that stood out was ionic polymer-metal composite (IPMC). IPMC is a material that displays artificial muscle behavior under an applied voltage or electric field. The UH team coated a flexible fish tail made of IPMC and applied a voltage to it using a power source to create a swimming motion as propulsion that mimics that of a fish.

Our group, Team M.U.D.K.I.P., initially wanted to build an aquatic soft robot that has depth control, jumping, and swimming. Building off Team Bay-Max's work, we are also working on utilizing reversible fuel cells for depth control. However, with our propulsion goals in the water, the buoyancy control devices must be smaller to reduce drag. Unlike last year's design, our robot aims to exploit another use case of fuel cells aside from just buoyancy control – jumping via combustion reaction of the H2 and O2 gas outputs from electrolyzer mode. By expanding the potential utility of fuel cells, we are increasing the likelihood of more sustainable technologies being adapted within spaces that can transition to greener operations. Initially, we planned to create a similarly shaped fish tail that can flex and have marine propulsion. Instead of being made of IPMC, our tail will be molded from flexible silicone and contain a hollow interior. This hollow interior was filled with gas on different sides depending on the direction in which we wanted the tail to flex for swimming. This combination of the three features was novel and would result in a unique soft robot that mimics mudskipper behavior; however, we determined later in the semester that the throughput requirements for the fish tail were too great, and instead appropriated the combustion mechanism for forward propulsion in addition to upwards propulsion.

Requirements

Our faculty sponsors, Dr. Laura Schaefer and Dr. Fathi Ghorbel, initially requested that the robot be capable of the following three requirements: 3-degree-of-freedom motion (rotation roll axis, rotation about the pitch axis, and depth control), continuous forward propulsion, and impulse forward propulsion or jumping. The 3-dof motion would be controlled by buoyancy control devices (BCDs), as was studied extensively by the previous design team, Bay-Max. The continuous forward propulsion would be controlled using a soft robotic fish-tail design (more on this design later). The impulse forward propulsion would be controlled using a hydrogen-oxygen gas combustion reaction that would propel the robot forward to resemble jumping (as that of a mudskipper).

The scope of these initial objectives was narrowed significantly, and Dr. Ghorbel reiterated new requirements that should allow us to circumvent the several technical issues that were hindering our team. Due to the technical problems with the BCDs, due to the clogging of the reversible fuel cells, as discussed in the Prior Work section, full-depth control was unable to be achieved. The fuel cells were successfully able to inflate the balloons. However, deflation of the balloons was unsuccessful. The fish-tail design was also placed on the back burner for now because the fuel cells we are working with were not powerful enough to generate the gas required to achieve meaningful forward motion via inflation and deflation of alternating sides of the tail (to result in a back and forth motion of the tail and thus forward propulsion of the robot).

Now, the primary focus of our design team and the new requirements for this project are as follows: use BCDs to achieve unidirectional depth control and rotation about the pitch axis, and use hydrogen-oxygen gas combustion to achieve horizontal underwater propulsion. Our final design will incorporate rotation about the pitch axis using BCDs so that we can orient the robot underwater so that there is at least a few degrees of angle between the front end of the robot and the horizontal axis. With this orientation, combustion will launch the robot forward, and due to the resisting force of the water, the robot will also be launched upwards. Thus, these two components will work in conjunction with each other to achieve a jumping motion resembling that of a mudskipper, which is the primary requirement as specified by Dr. Ghorbel.

The official budget for this project, as funded by the OEDK, is $2,500. We plan to boost this amount via external funding sources. We were also informed by Dr. Ghorbel that the budget for this project is flexible, and we may be able to exceed the set amount if deemed necessary to gather the required fuel cell components and other parts.

Engineering Standards

EHS Standards:

To carry out the hydrogen-oxygen combustion test, the team needed to clear our procedures with the Rice University Environmental Health and Safety (EHS) Department. Our Standard Operating Procedures (SOP) for this test were developed in line with the practices required by Rice EHS as specified on their website[6]. Our faculty sponsors, Dr. Laura Schaefer and Dr. Fathi Ghorbel, approved our SOP document and gave us their signatures. We then cleared our SOP through Rice EHS. The document was created to ensure the safety of all individuals who will experiment with the combustion of Hydrogen and Oxygen gas housed within a pressure vessel. It is specifically geared towards testing gaseous fuels produced from electrolytic fuel cells. The instructions for the combustion test, as stated on the SOP, are listed below verbatim:

1. Collect and assemble all essential components for combustion testing:
    - PEM fuel cell
    - Wires
    - Elastic tubing
    - Battery/power source
    - Spark plug
    - Combustion Chamber
    - Syringe
    - Distilled water
    - Pressure vessel to contain the explosion
    - Rails
    - Sensors
2. Ensure the spark plug is not connected to power.
3. Turn on the fuel cell and observe the production of gas.
4. Check plumbing connections and ensure there are no leaks.
5. Turn off the fuel cell and release gas within the pressure vessel.
6. Stand approximately 35 feet away from the test setup.
7. Connect the spark plug to the power.
8. Turn on the fuel cell and wait till the predetermined amount of fuel is produced.
9. Turn off fuel cells.
10. Ignite the spark plug, propelling the device across horizontal guide rails.
11. Wait for the device to stop.
12. Disconnect the spark plug from the power.
13. Spray a carbon dioxide fire extinguisher over the site to extinguish difficult-to-see flames.
14. Inspect the test setup for any significant damage.

Our work on these safety procedures was also informed by the General Environmental, Health, and Safety (EHS) Guidelines documents. These are technical reference documents with general and industry-specific examples of Good International Industry Practice (GIIP).[8] These guidelines were also developed in conjunction with relevant Industry Sector EHS Guidelines, which guide users on EHS issues in specific industry sectors. To reduce the impacts of our tests on the surrounding environment, we ensured that the overall experiment resulted in zero emissions. The sole byproduct of combustion is heat and water, most of which is dissipated shortly after experimentation. We also ensured no foliage was present in the general vicinity of the combustion chamber. The area, Rice South Annex, primarily used for testing, is not an ecologically sensitive location. Overall, our practices had no impact on the testing location's environment.

ASME Standards:

Our design project and the testing setup for our experimental procedures were established in line with the engineering standards established by the American Society of Mechanical Engineers (ASME). In addition to having followed the safety standards of Rice EHS, we also used safety practices and regulations defined by the ASME to guide our experimentation. This work was informed by the NFPA 54: National Fuel Gas Code (Current Edition: 2015). This is a safety code that applies to the installation of fuel gas piping systems, fuel gas utilization equipment, and related accessories. Coverage of piping systems extends from the point of delivery to the connections with each gas utilization device. For systems other than undiluted liquid propane gas (LPG), the point of delivery is considered the outlet of the service meter assembly, the outlet of the service regulator, or the service shutoff valve where no meter is provided.[7] In addition to other safety codes published by the ASME, our work was well within the regulations of the codes specified by this nationally recognized institution.

Design Process

Activities Completed

For the activities of the past semester, we spent the majority of the first month researching and brainstorming fuel cell design. Once we arrived at solutions we liked, we moved forward with the following activities. We went to the University of Houston to visit a research lab that Dr. Ghorbel is working with. They study fuel cells and their applications in buoyancy control devices (BCD). This meeting was extraordinary. We got to see the exact model of the fuel cell we were using in action. We spent considerable time interacting with the graduate students running this research. Our questions allowed us not to learn through trial and error. Instead, we used the interaction to compress a portion of his years of experience working with fuel cells. We gathered inspiration from their fish design. This led us to focus on the fishtail design. After researching biomimicry robotics, we found an MIT research group that created a soft fishtail using pressurized gas. We found this paper and modeled our work after theirs. We made the CAD model of our tail. We printed the model. We poured the silicone into the mold, and then we had our tail. We then spent considerable time researching and analyzing the combustion chamber setup. We worked with Ansys to develop a modeled simulation of the explosion. We considered a variety of ways to create a safe combustion reaction that would propel our robot into the air. We made multiple CAD models of this and printed them to learn their feasibility. There was also a significant focus on the safety of the combustion. We spent considerable time selecting the right fuel cell, as it was undoubtedly the most expensive part of our robot. We also considered building our fuel cell, but that would be a senior design project on its own. We found great difficulty finding a reversible fuel cell that would produce hydrogen and oxygen at a rate we favored. Once we selected the design, we began thoroughly testing it. We became very familiar with the fuel cell. We learned how it works, how to set it up, and the electrochemistry behind it. We also needed to test the combustion itself. Before we can add a combustion chamber to our robot, we need to have data on it. This took the most significant amount of time. We meticulously thought through the safety protocols of the combustion. We worked with EHS to make sure it was safe. Unfortunately, EHS, the committee in charge of permitting us to launch, stopped responding to our emails. This created a multi-week delay in our testing. Once we were finally able to test, we had our testing setup planned, prepared, and ready. Unfortunately, at our first iteration of testing, the combustion chamber never launched. We concluded there was either an issue with the production of gas or the ignition itself. We improved our gas production, reduced leaks where we could, and improved our ignition system. After two more iterations of unsuccessful combustion, we finally had a successful combustion. Our setup included a syringe instead of a water bottle setup. This allowed for a purer combination of hydrogen and oxygen gas. With this and the new reduced scope of our project, we have reached a successful approach to our robot.

Research

Researched Fuel Cell Design

In our initial research, we found various types of reversible PEM fuel cells. One of the most prominent vendors is Fuel Cell Store, where we eventually bought a lot of equipment for our project. We read through their articles on the different layers that go into a reversible fuel cell, such as the sealant, gasket, gas diffusion layers, catalyst, membrane, and more. We even considered purchasing the layers separately to assemble ourselves into a reversible fuel cell. This would give us more flexibility to create a reversible fuel cell with a unique catalyst for faster reactions or just have a larger surface area overall for more gas production. After consulting with our advisors, we decided that this was a risky move, as a lot could go wrong when making our membrane electrode assembly (MEA). We ended up purchasing a double reversible fuel cell from their website, which has two MEAs in parallel for faster production. Later, to our dismay, we realized that oxygen was not sufficiently collected in our syringes during electrolyzer mode because the specific design had holes where air is usually an input while operating in fuel cell mode. These holes were on the oxygen side, and thus most of the oxygen escaped while the hydrogen didn't, creating a non-ideal gas ratio for combustion.

Researched BCDs

Through our research, we found information on BCDs, but it still wasn't plentiful, as the interest in reversible PEM fuel cells at our scale is not widely used or researched. Because of this, we decided to work on improving the BCD design from Team Bay-Max by using better coupling inside and minimizing the size of the overall BCD. This is essential for our robot to swim well when combusting, as the new design would minimize drag.

Discoveries through experience/prototyping

During our early research on hydrogen-oxygen combustion, we discovered a microrobot developed by Wiss Institute and Harvard's SEAS. This robot leveraged electrolysis to produce hydrogen and oxygen, propelling the small robot out of the water. The fuel mixture was contained within a cubic chamber, open at the bottom, which interfaced with the water to create air space to house the propellant.[4]

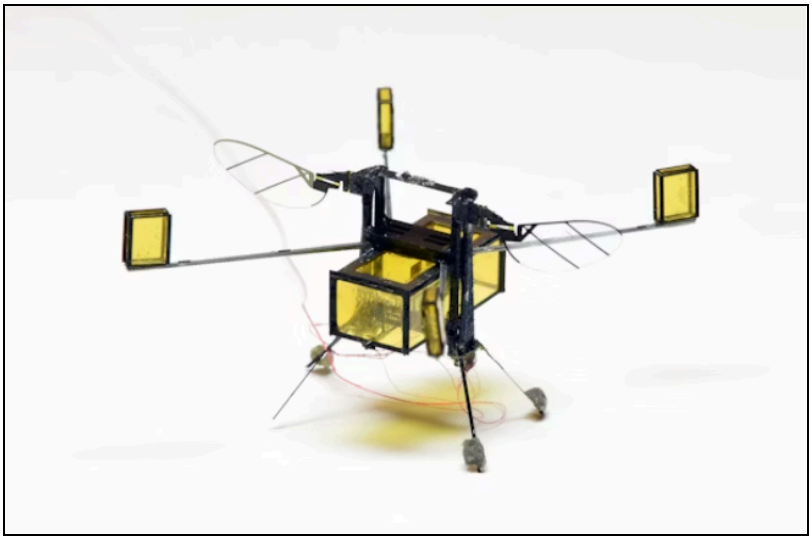

Figure 1: Aerial-Aquatic Microbot from Wyss Institute and Harvard's SEAS

Notably, the research group successfully proved the viability of gaseous hydrogen-oxygen propulsion at a micro-scale. The significant difference between our work on combustion boils down to a difference in the magnitude at which this gaseous fuel is viable for propulsion. Our robot will ultimately consist of three buoyancy control devices (BCDs), various heavy electronics, and a combustion chamber. We must conduct multiple experiments to fine-tune the capabilities of using this fuel mixture to propel a small to mid-sized robot.

Rejected ideas

After meeting with Dr. Ghorbel towards the end of the semester, a significant design change was made. He reduced the scope of our project. As our project is quite ambitious, his request was narrowed. Initially, we were focused on a robot that could swim in the water with 3 DOF swimming capabilities and was capable of jumping out of the water into the air when it was at the surface of the water. We were also expecting to add gliding capabilities if we had additional time. However, after a discussion with Dr. Ghorbel, he narrowed our scope to the following. We are now using combustion to propel us forward in the water and use our BCDs to guide the motion from the water to above the surface of the water.

The tail design had to be placed on hold for multiple reasons, but most obviously, a fuel cell does not have the flow rate or pressure to make the fishtail propel the robot forward in the water. Even if we reduce the size of the fishtail, reduce the thickness, and increase the elasticity of the material, we would still need a rate of hydrogen and oxygen gas production that our current electrolyzers can't supply. This means that even if the fishtail is as favorable as we want it, it can't propel our robot forward as it is limited by the fuel cell.

Skills learned

CAD

One of the team members, Lucas, has extensive experience working with CAD, so through the BCD and robot design, he was able to show Andrew how to navigate the software. Together, they modeled the fuel cell on SolidWorks as an introduction to CAD. Andrew learned how to make sketches, use constraints, dimensions, features, tools, and some good workflows for using CAD software.

Ansys

While exploring software to model our combustion process, we turned to Ansys Fluent in hopes of simulating fluid flow. Unfortunately, after some discussion with Rice Eclipse as well as trial and error within Ansys, we learned that we simply could not model our system dynamics within the software. This boiled down to our combustion occurring instantaneously, so fluid flow happened in a fraction of a second. This differed from traditional rocket propulsion since they typically have sustained fluid flow from constant fuel injection.

CEARUN

CEARUN is a software by NASA that calculates the properties and compositions of chemical equilibria for complex mixtures, and one of its explicit purposes is to run combustion reaction simulations, which helps us to analyze our combustion process in stages.

Soft Robotics + Fish Tail

To create a similar fish tail like the one MIT had in their paper, we had to 3D print casting molds for the silicone tails. Two different molds were printed – one for the middle layer that separates the two chambers for movement, and one for the outer layer of the fishtail. Imperfections in our first few tails improved our overall molds, and we were finally able to create a sturdy tail whose parts were “glued” together by dried-up silicone. The flexibility of the tail was demonstrated with a high-pressure bicycle pump, and we could observe the swimming motions.

Ignition

The key to a reaction is a spark, flame, or energy source that kicks off the H2 and O2 gas combustion. In our case, we found that generating a spark was the safest option. We

started with piezoelectric igniters that would generate a small spark upon a considerable applied pressure. This was later scrapped due to the immense force needed to push down, which is fine when a human does so, but will eventually become difficult when it needs to be moved remotely. After some more research, grill igniters were chosen. These are typically used to generate a spark to ignite the propane, and it didn't take much force to press. We purchased it and eventually connected the prongs to 30-foot-long wires that we cut off a rocket controller launcher via alligator clips. This proved successful at generating the spark in our numerous combustion tests. However, the distance of the prongs is crucial for electrons to jump across the gap from one prong to another, especially at lower voltages. With such long wires, even the amplified voltage from the grill igniter suffered a sufficient voltage drop, to the point where we had to tape the ends closer together, leaving around 0.25 mm of gap. At our fall semester presentation, Dr. Woods suggested using spark plugs to generate the spark. We had considered it previously but ignored it in favor of the grill igniter design. Given that our current setup has limitations and that spark plugs are intentionally meant to create sparks using very high voltages, we will look into this method more in the spring.

Fuel Cell Electrochemistry

The fuel cell electrochemistry can be pretty complex, but for our task, the idea is quite simple. We are using PEM fuel cells. Applying hydrogen gas to one side of a membrane and oxygen gas to the other side of the membrane will produce water and electricity. Electrolyzers work in the opposite direction. They take in water and electricity, and they output hydrogen gas and oxygen gas. There are also reversible fuel cells that perform both actions, but both processes are limited as they can not be optimized in both directions due to each process having a preferred catalyst. Furthermore, the fuel cell mode operates about ten times slower than the electrolyzer mode in terms of gas exchange. Electrolyzer mode was also observed to be hindered by fuel cell mode when the water clogged up the tubes. Since there was not sufficient pressure from the gas produced to push the water out, it just stayed stuck in the tubes until we had to intervene. There is a lot of documentation for the industrial-level usage of fuel cells, but there is very little documentation for fuel cells and electrolyzers on the scale we are using them.

Manufacturer Communication

The key components of our design are electrolytic fuel cells. This meant we had to conduct thorough research to find fuel cells best suited for our project requirements. Next, we contacted fuel cell distributors/manufacturers such as Horizon Fuel Cells and The Fuel Cell Store for the following: requested data sheets on fuel cell specs, and sought advice from sales engineers who understood their vast inventory of products.

Usage of Previous Coursework

Proton Exchange Membrane (PEM) Fuel Cells:

A schematic detailing the mechanics of how Proton Exchange Membrane (PEM) fuel cells operate is shown in Figure 2 below. Here, we can see that when hydrogen gas (H_2) is provided on one side and oxygen gas on the other (ideally pure O2, but air can also work with a cost in efficiency), water can be produced in conjunction with electricity. If a reversible fuel cell is used, the reverse, electrolysis, process can also be executed, where pure deionized H_2O is separated into H_2 and O_2 gases when the reversible fuel cell is supplied with electricity. It is also important to note that when the fuel cell is operating in these modes, the water and oxygen gas are on the same side of the fuel cell. It is essential to understand this when implementing this device in other systems, as detailed in different sections of this document.

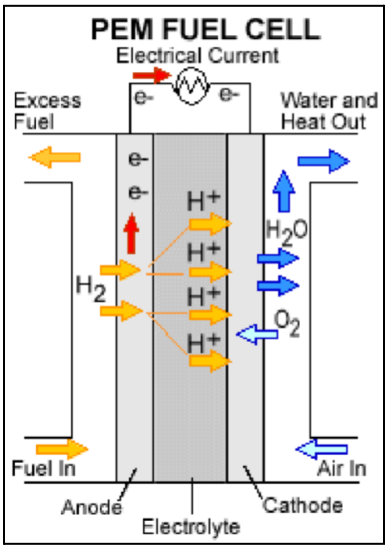

Figure 2: PEM Fuel Cell Schematic [Schaefer - MECH 477 - 3-3]

The chemical reaction of the PEM fuel cell shown above, when operating in the fuel cell mode, is detailed in the chemical equations below.

$$\text{Cathode: } \tfrac{1}{2}O_2 + 2\,e^- + 2\,H^+ \Rightarrow H_2O$$

$$\text{Anode: } H_2 \Rightarrow 2\,H^+ + 2\,e^-$$

$$\text{Overall: } H_2 + 1/2\,O_2 \Rightarrow H_2O$$

Microprocessor programming

The ELECs did not have too many skills applied from their major-specific classes, but Arduino and general microprocessor programming skills were needed, which we learned in ELEC 327 junior lab. Initially, we set up ultrasonic distance sensors for velocity and acceleration calculations of the water bottle immediately after the combustion reaction. It worked well, and we generated live plots of the detected distance versus time. However, the sample rate of one ultrasonic distance sensor is not nearly as fast as we would like it to be, and setting more than one up to increase the overall sample rate just seemed too sophisticated and unreliable. We ended up checking out a 120 fps camera from the Digital Media Commons to record our combustion reaction. We also had to actuate a servo we bought for general-purpose cases. In the spring, we might use the servo to deploy a glider either in the water or in the air. Ideally, a signal would be sent from our laptop to the microprocessor over WiFi, since the appropriate time for glider deployment is hard to approximate via code.

Adiabatic Flame Temperature (Thermodynamics)

Assumptions:

- The chamber in our model was adiabatic in which no heat transfer occurred through its walls, and instead, all of the heat went into heating up the water vapor product of the combustion reaction.
- Perfect combustion was achieved in which the oxygen from the electrolysis reaction provided the theoretical amount of air necessary to react 100% of the reactants (Hydrogen and Oxygen) and produce 100% of the products (water vapor)
- The Hydrogen, Oxygen, and water vapor can be treated as ideal gases throughout the entire process..

Process

- By using the equations below,, learned from the Thermodynamics textbook, we were able to approximate a maximum value for the force exerted by the combustion reaction onto our testing setup.
- We first calculated the enthalpy of the water vapor produced in our combustion reaction by manipulating **equation 1** to solve for enthalpy (**equation 2**) and finding its temperature using an iterative process relying on **equation 3** and values from online tables. Then that temperature was used to calculate the pressure of the water vapor using the ideal gas law **(equation 4)**. Lastly, the pressure and known area of our syringe chamber were used to calculate a maximum force value **(equation 5)**.

$$\mathbf{\Sigma} n_{products}(h_f + \Delta h)_{products} = \mathbf{\Sigma} n_{reactants}(h_f + \Delta h)_{reactants} \quad (1)$$

$$h_{water,T_{final}} = \frac{(n_{oxygen}\Delta h_{oxygen} + n_{hydrogen}\Delta h_{hydrogen} - n_{water}h_{f,water})}{n_{water}} + h_{water,273} \quad (2)$$

$$h_{water,T_{final}} = c_v T_{final} \quad (3)$$

$$P_{final} = \frac{n_{water} RT_{final}}{V_{syringe}} \quad (4)$$

$$F_{thrust} = \frac{P_{final}}{A} \quad (5)$$

Old State of the Project (Fall 2024)

Explosion setup

Given the dangerous nature of our design challenge, our team immediately recognized the importance of developing a test stand that could safely restrain our combustion experiments. The key features that we looked for are repeatability, modifiability, portability, and safety. The test stand took the form of two guide rails that interface with each other through a 3D-printed fixture. These guide rails are fastened to two wooden planks through bearings that enable the test stand to be elongated or shortened. Another 3D-printed fixture was then bolted on top of the component that interfaces with the guide rails. This top component, depicted in red as seen in the image below, enables combustion chambers of different dimensions to be securely zip-tied onto the test stand. All in all, the test stand weighs 10 lbs, can be expanded laterally by 3D-printing wider components, and enables the user to test combustion chambers of varying sizes.

When arriving at the testing site, South Annex, the team would secure the test fixture to the ground by using stakes that were driven through the planks secured on the bottom side of the test stand. Next, we would set our fuel cells to begin filling the combustion chamber with hydrogen and oxygen gas as depicted in Figure 3 below. Check valves were used between the fuel cell and the combustion chamber to prevent the backflow of gas. Furthermore, we used various methods to seal off the combustion chamber from the atmosphere once it's done filling. For instance, we used clamps, wooden plugs, and check valves to prevent fuel from leaking.

Next, we utilized the Sony Mirrorless Camera a6300 and a6400 to record our combustion footage since its 120-frame rate capability is higher than what our time-of-flight sensors are capable of.

Lastly, different ignition methods were attempted to spark our fuel to combust. For instance, we tried to short-circuit a battery, but the minimum safety distance required for ignition was long enough to prevent a spark from being produced. Therefore, we opted for a completely wireless remote start through the use of a prebuilt transformer and wifi from an Arduino.

Figure 3: Filling the Combustion Chamber with Fuel

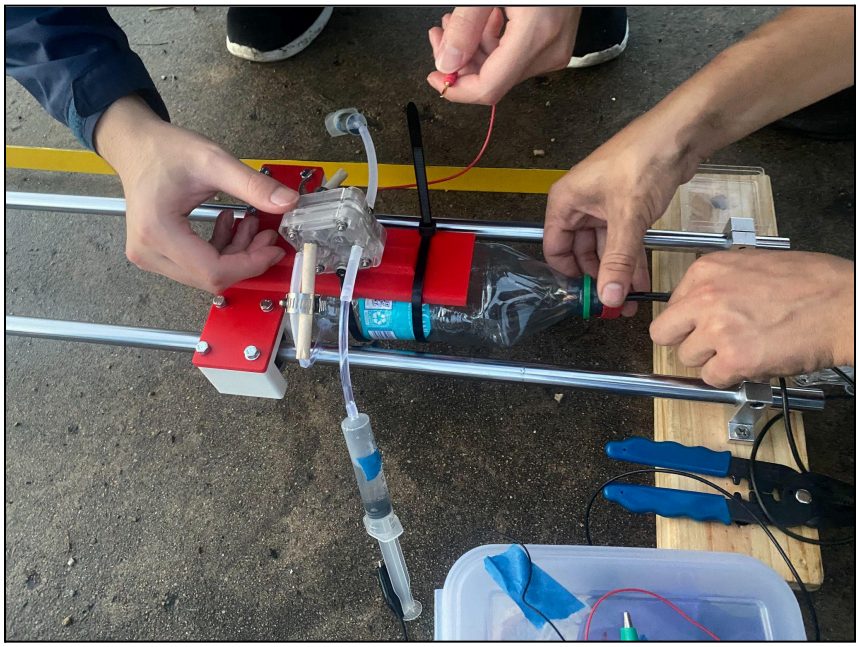

Figure 4: Combustion Test Setup

Figure 5: Sony Mirrorless Camera a6300 a6400

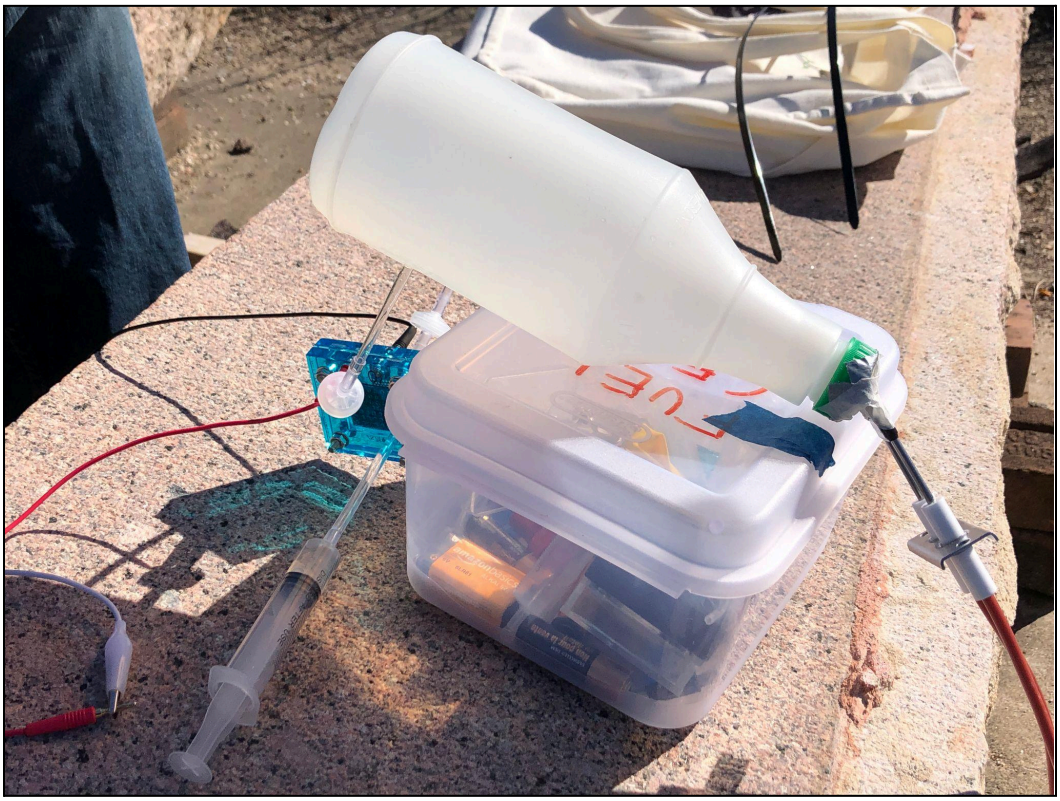

Figure 6: Our latest combustion chamber that features a drilled-out bottle cap where we insert the igniter

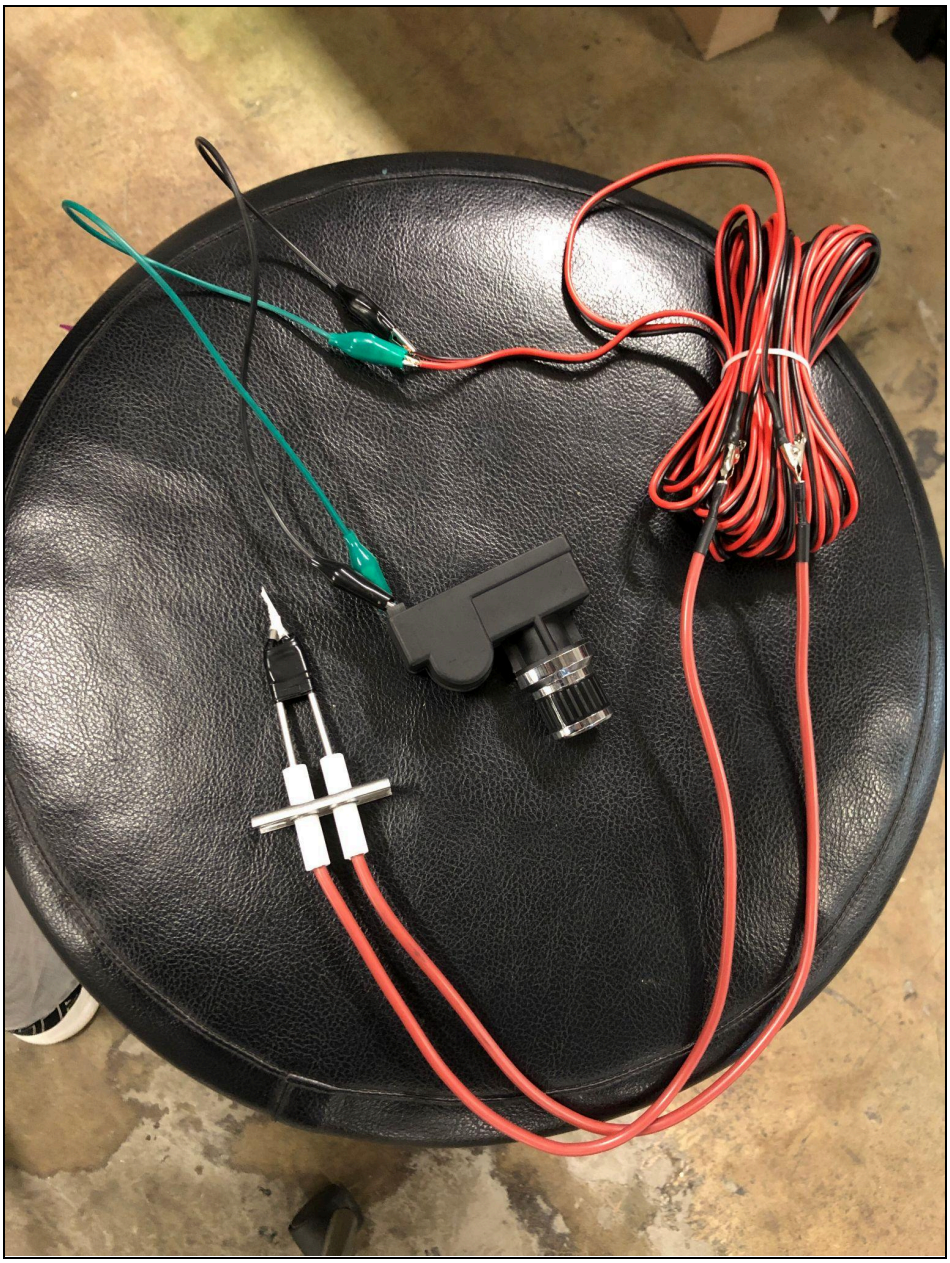

Figure 7: Our latest ignition mechanism that is capable of extending over 30 feet

The biggest issue we faced was simply not achieving combustion within our chamber. This problem can be derived from various components not performing as intended. For instance, the team initially used a double reversible, as seen in Figure 4, that did not produce consistent amounts of oxygen. Initial testing showed the correct performance of the cell, but after extended testing, we concluded that there was inconsistent production of oxygen. Therefore, we reverted to using the educational fuel cells from Horizon since these were extensively tested, and we are confident in their consistent gas production.

Another issue was that our first low-fidelity combustion chamber consisted of a bottle made of polyethylene terephthalate. Hot glue was also used to seal areas with potential leaks. This design is not optimal due to the permeation of hydrogen through these materials. Therefore, the bottle was substituted with one made of polyurethane, which can act as a barrier against hydrogen gas diffusion. Additionally, hot glue was also substituted with epoxy.

Combustion Chamber Design

The initial design of the combustion chamber had to account for the following variables: repeatability, underwater/above-water combustion, and a mechanism to prevent backflow. The idea for allowing underwater combustion while preventing water from entering the combustion chamber is a one-way valve. This device would allow the flow of exhaust gas but avoid the flow of water inward. The downside of this mechanism is the significant losses associated with the fluid flow through a valve.

To ensure we knew the exact fuel-to-oxidizer ratio we were handling, we decided to create a vacuum within the combustion chamber. To do this, we attached a vacuum flange to the chamber and connected a hand pump to the system. In testing, we would pump as much air out of the chamber as possible to get our fuel mixture close to stoichiometrically perfect. Internally, the combustion chamber would have plumbing at both ends of the hydrogen and oxygen ports. This plumbing would be unique in that each tube would have holes across its length. This would mimic the function of an injection plate within a rocket engine. By mixing the hydrogen and oxygen gases, we can improve the burn efficiency of our fuel.

Following our meeting with Dr. Ghorbel, the team had to simplify our design to ensure we met our new combustion goal. This shift in our design consisted of creating a combustion chamber that can function both above water and underwater for a single use. Taking what we learned from our first chamber design, we developed a chamber that functions similarly to a syringe. This new chamber would exploit the method of a syringe, creating a vacuum to ensure a perfect fuel mixture. Additionally, we no longer worry about water or air entering our chamber after combustion since our device is designed to function as intended once.

Combustion Analysis

Theoretical analysis was conducted on the hydrogen-oxygen combustion in conjunction with experimental results. Below, the theoretical analysis of the combustion and the force generated by the impulse is shown.

Mechanics

$$F_{Net}(t) = m * a(t)$$

$$F_{Net}(t) = F_{Thrust} - F_{Friction} - F_{Drag}(t)$$

$$F_{Thrust}(t) = m * a(t) + F_{Friction} + F_{Drag}(t)$$

$$F_{Net} = m * a$$

$$F_{Net} = F_{Gravity} - F_{Friction} - F_{Drag}$$

$$F_D = \frac{1}{2} C_D A \rho V^2$$

Solve for C_D

$$F_f = \mu F_N$$

$$\mu \approx 0.0015$$

Bearing Type	Coefficient of friction - μ
Deep Groove Ball Bearing	.0015
Angular Contact Bearing	.0020
Cylindrical Roller Bearing, Cage	.0010
Cylindrical Roller Bearing, Full Comp.	.0020
Tapered Roller Bearing	.0020
Spherical Roller Bearing	.0020
Ball Thrust Bearing	.0015
Cylindrical Roller Thrust Bearing	.0050
Tapered Roller Thrust Brg, Cage	.0020
Tapered Roller Thrust Brg, Full Comp	.0050

Frictional force would simply be: Force = P x μ

Table 1: Coefficient of Friction for various ball bearing types[9]

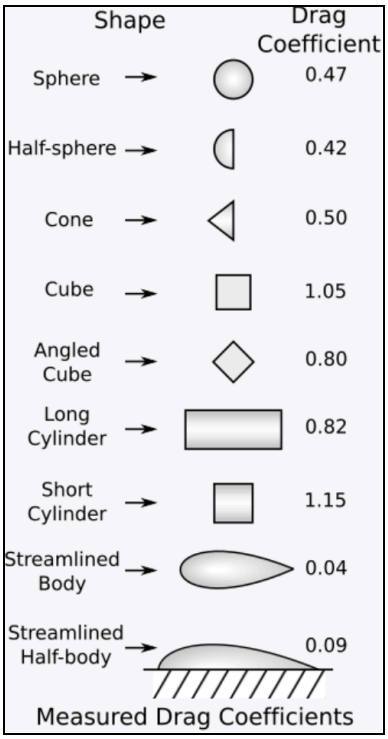

Table 2: Coefficient of Drag for various geometric shapes

Experimental Analysis

The experimental analysis was conducted on the third successful combustion trial. Figure 8 below shows the Tracker software that was used on the video footage of the successful combustion test. This software was used to gather experimental data on the kinematics of the test, such as the position, velocity, and acceleration of the rig after the combustion. These values are tabulated in Table 3. These values can then be implemented into the theoretical analysis detailed previously, and values can be compared.

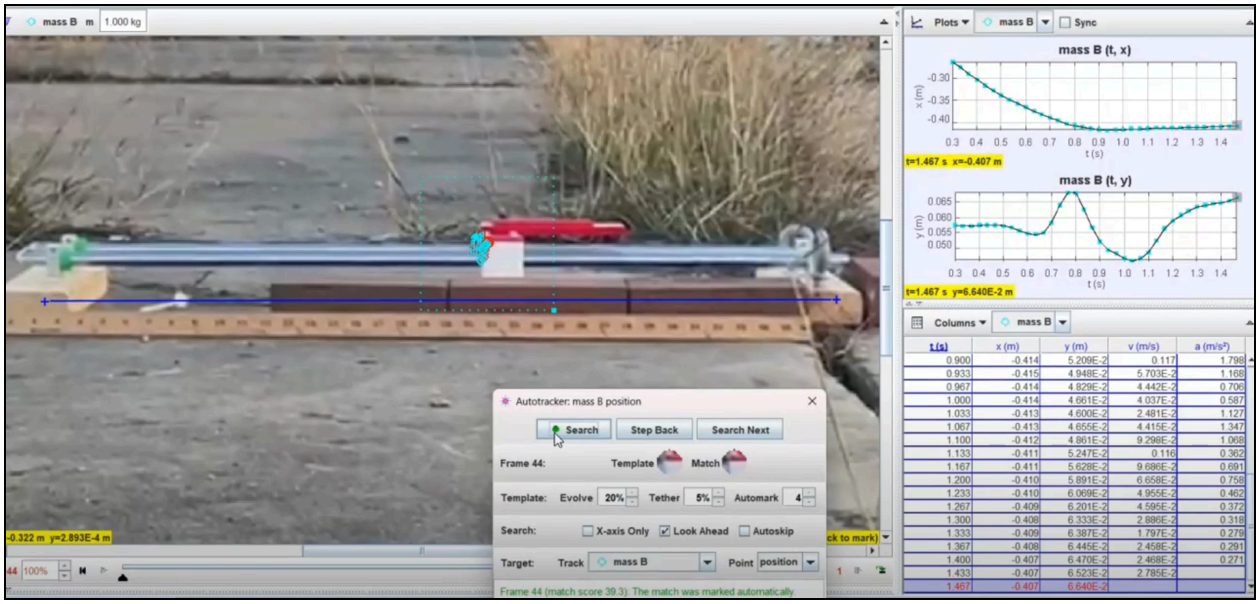

Figure 8: Tracker software used in video footage to gather experimental data on the third combustion test

t (s)	x (m)	y (m)	v (m/s)	a (m/s²)
0.300	-0.263	5.740E-2		
0.333	-0.276	5.726E-2	0.396	
0.367	-0.290	5.715E-2	0.408	0.133
0.400	-0.303	5.739E-2	0.384	0.662
0.433	-0.316	5.752E-2	0.366	0.825
0.467	-0.327	5.746E-2	0.331	0.916
0.500	-0.338	5.733E-2	0.302	0.939
0.533	-0.347	5.663E-2	0.278	0.565
0.567	-0.356	5.560E-2	0.263	0.305
0.600	-0.365	5.479E-2	0.263	0.547
0.633	-0.374	5.441E-2	0.244	1.433

Table 3: Kinematics of the third experimental combustion test

Fishtail Design

The primary method with which our team initially planned to incorporate continuous forward motion (not impelled by combustion) via reversible fuel cell technology was using a fishtail bio-inspired soft robotic design. This design was inspired by a research study published by an MIT research group. From Figure 9 below, we can see the mechanics behind how this design works.

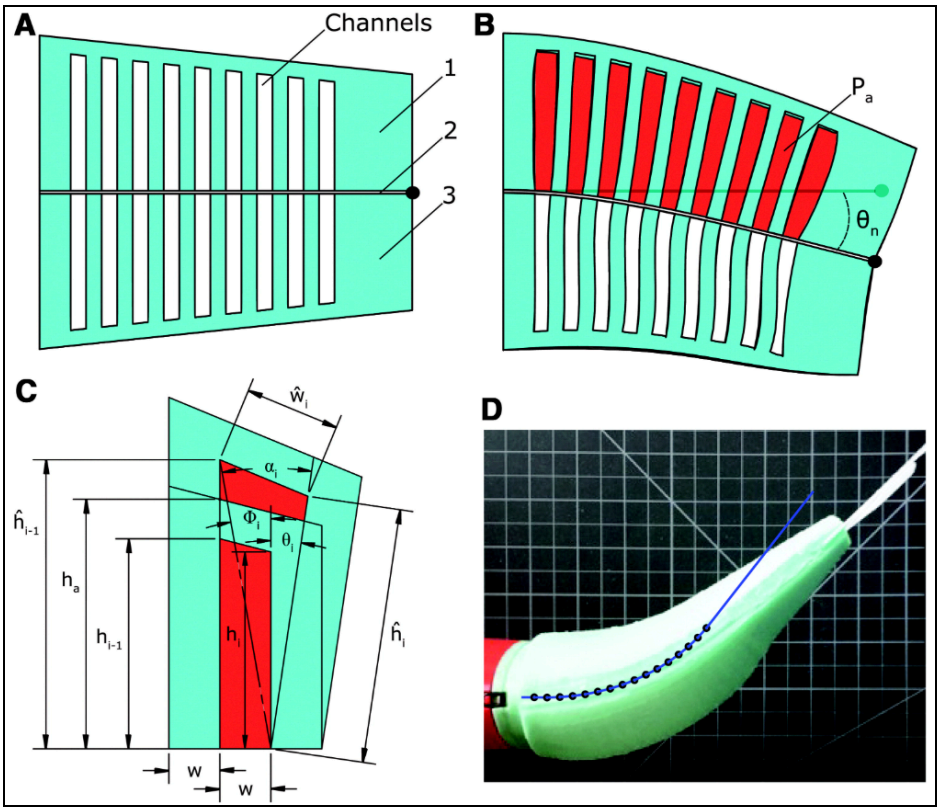

Figure 9: Schematic representation of a tapered bidirectional FEA in cross-section. (A) The three-layer structure: symmetric agonistic (1) and antagonistic (3) expanding layers sandwiching an inextensible but flexible constraining layer (2). Here, embedded channel groupings are in a depressurized state. (B) Pressurized gas (red) expanding the agonistic channel group. Because of the constraining layer, fluid pressure induces a bending moment, producing curvature. (C) Model parameters. (D) Predicted curvature of the fish's anterior actuator overlaid atop the actuator's actual deformation. FEA, fluidic elastomer actuator.[2]

In the MIT design, they were able to achieve forward propulsion using this method by inflating one side of the tail with pressurized gas while vacuuming the other side of the tail. This would cause the tail to bend in one direction. When the inflation and deflation were reversed, the tail would bend in the other direction. Repeating this cycle would cause the tail to paddle back and forth and result in the forward motion of the robot.

We intended to use this design in our robot, except instead of powering the inflation and deflation of the tail using valves and pressurized gas, this process would be powered via reversible fuel cell technology, as we want the entire robot to be passively actuated (no active mechanisms such as valves, pumps, or motors). The theoretical idea was that the reversible fuel cell would produce oxygen and hydrogen gas when operating in the forward mode, thus inflating the tail, and it would turn those gases back into water when operating in the reverse mode. In Figure 10 below, the molds used to create the physical prototype of our design are shown.

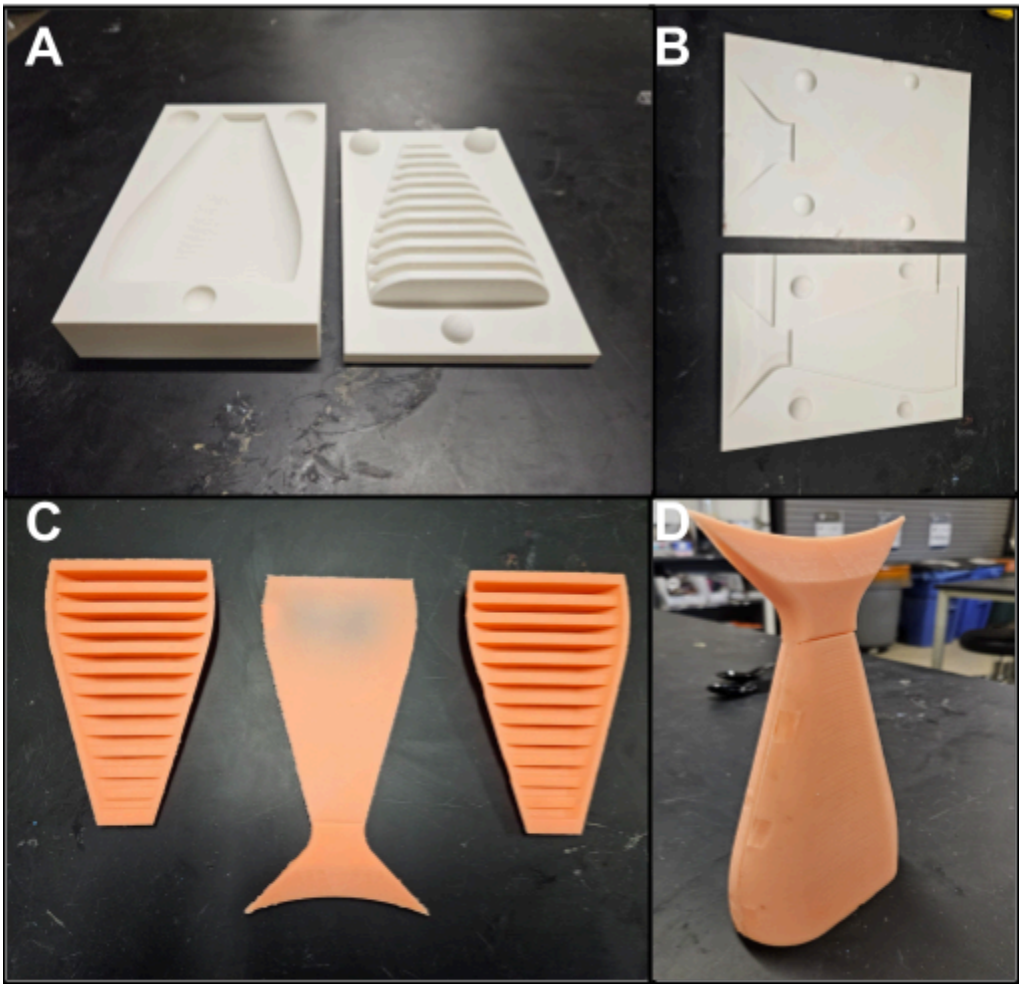

Figure 10: (A) 3d printed PLA mold for the tail side. (B) 3D printed PLA mold for the middle section of the tail. (C) Smooth-On Rebound 25 silicone molded pieces of the fishtail. (D) Completed soft robotic bio-inspired fishtail prototype.

After prototyping the fishtail, it was tested using a tire pressurizer. In Figure 11 below, the preliminary test of the tail pressurized via a tire pump is shown. The pressure required to achieve this level of deformation in the tail was a maximum of 5 psi.

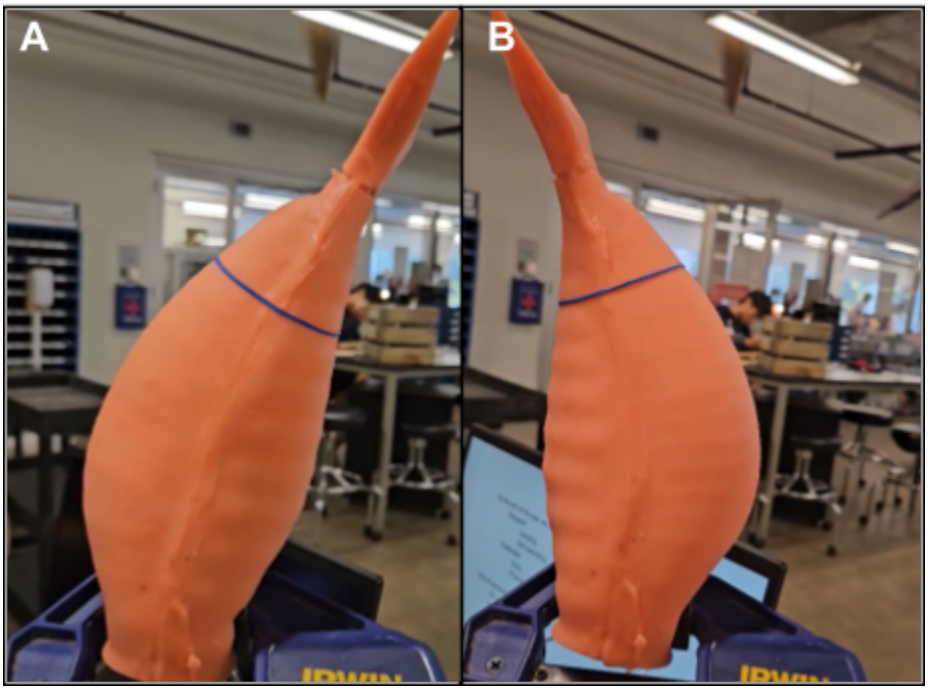

Figure 11: (A) Inflation of the left side of the tail using the tire pressurizer at five psi to move the tail to the right. (B) Inflation of the right side of the tail using a tire pressurizer at five psi to move the tail to the left.

Because it would require a significant amount of time for a fuel cell to produce enough gas to generate a pressure of 5 psi, improvements needed to be made to increase the flexibility of the soft robotic fishtail, theseimprovements included downsizing the tail, increasing the number of chambers within each side of the tail, reducing the relative thicknesses of all the walls, and using more flexible silicon (such as Smooth-On EcoFlex 10) so that it would be less rigid than the initial prototype shown in the previous figures. Eventually, the fishtail design was set aside to be looked at later so that we could prioritize more crucial aspects of the required finished product as requested by Dr. Ghorbel. If time permits, however, we would like to return to this design and see if we could implement our suggested improvements and perhaps power the tail's motion with purely reversible fuel cell technology.

Preliminary Robot Setup Overview

Given that we wanted to make our design as simple as possible, we decided to have it consist of 4 main components: the Central Body, BCDs, Branches, and Combustion Chamber.

The main body of our robot would be a waterproof and aerodynamic structure that can comfortably house all electrical and control components (microcontroller/PCB and power source) and any additional fuel cells and electrolyzers connected to our combustion chamber. Our current design will be composed of a waterproof resin material base and a pill-shaped housing, as well as all hardware.

Previous designs of the Buoyancy Control Device (BCD) framework revolved around a 4-unit structure capable of controlling rotation around the x and y-axis and motion in the z-axis. To improve that design, we plan to create a 3-unit cell framework with the same degrees of freedom while allowing for a simpler and lighter design. We also plan to make the unit cells smaller to minimize wasted space. The first iterations of the BCDs will also be made of waterproof resin material. They will be around the central body and form a triangular configuration.

To reduce excess surface area contributing to drag in the z-axis of motion, we want to connect the BCD unit cells to the central control body of the robot with cylindrical branch structures rather than a flat body. This design would also give the design larger moments for the arms to rotate around the x and y axes, requiring less force and thus less gas from the fuel cells. Additionally, the branches would house the wiring and tubing and connect them from the main body to the BCD unit cells. We plan to manufacture the branches with aluminum to maintain structural integrity and stay lightweight.

The combustion chamber will consist of a syringe-like mechanism attached to the edge of the triangular structure. It will be set up to take in the hydrogen and oxygen necessary to combust and propel the robot forward in water.

A special consideration for our design is that it must be as aerodynamic as possible to maximize the amount of underwater propulsion we can achieve for each combustion reaction. To accomplish this task, we are planning to add a triangular wrap-like structure that surrounds the other components. This will allow the robot to be more aerodynamic when moving in the x and y axes without increasing drag in the z-direction.

Preliminary Robot and BCD CAD Designs

The following is the setup of the BCD. We are interested in creating housing for the BCD with a streamlined shape for aerodynamics. The syringe will have a slot that directly fits into the BCD. The BCD will be held together with an O-ring and will be made of resin, and it will be sprayed with a resin to reduce the likelihood of leakage.

Figure 12: Setup of the new BCD to minimize volume and optimize aerodynamic shape

This brings us to the new design of the robot. Once the BCDs are placed in a triangle setup, we can attach them to the center “pill” which houses the electronics and provides structure to the robot. This triangle shape allows for better control of the 3-dof swimming with one less BCD than a quadrant of BCDs. The triangle strip that surrounds the robot allows for more streamlined swimming in the forward direction and does not add a lot of drag when moving up and down.

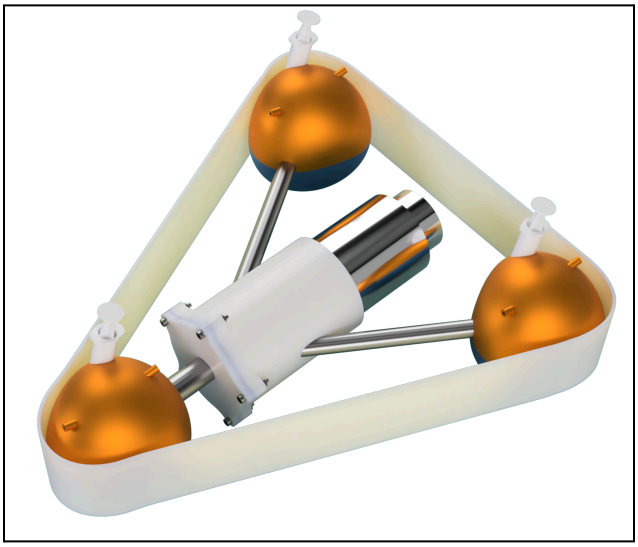

Figure 13: The entire desired robot with the triangle of BCDs, pill, and the triangle stip

Taking a closer look at the pill, we can find a 3D-printed plastic cylindrical container with an O-ring to house the electronics. This may be an issue as a 3D-printed container is not fully waterproof. We would also use the beams connecting the BCDs to the pill as tubes to connect the wires from the BCD to the pill.

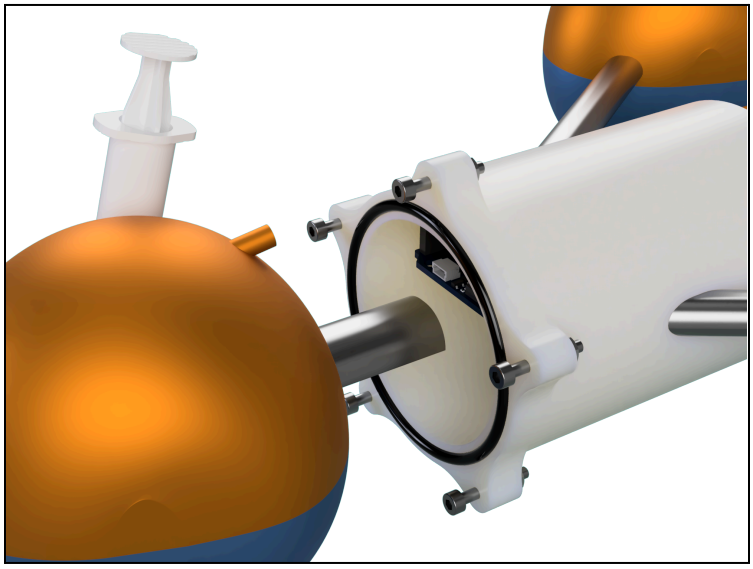

Figure 14: The electronics housing inside the Pill

As we can see in Figure 15, the combustion chamber will have the same piston cylinder usage, but it will be made of aluminum 6061. We chose this material as it is strong enough to hold our explosion, but light enough not to make a very significant impact on our robot's mass.

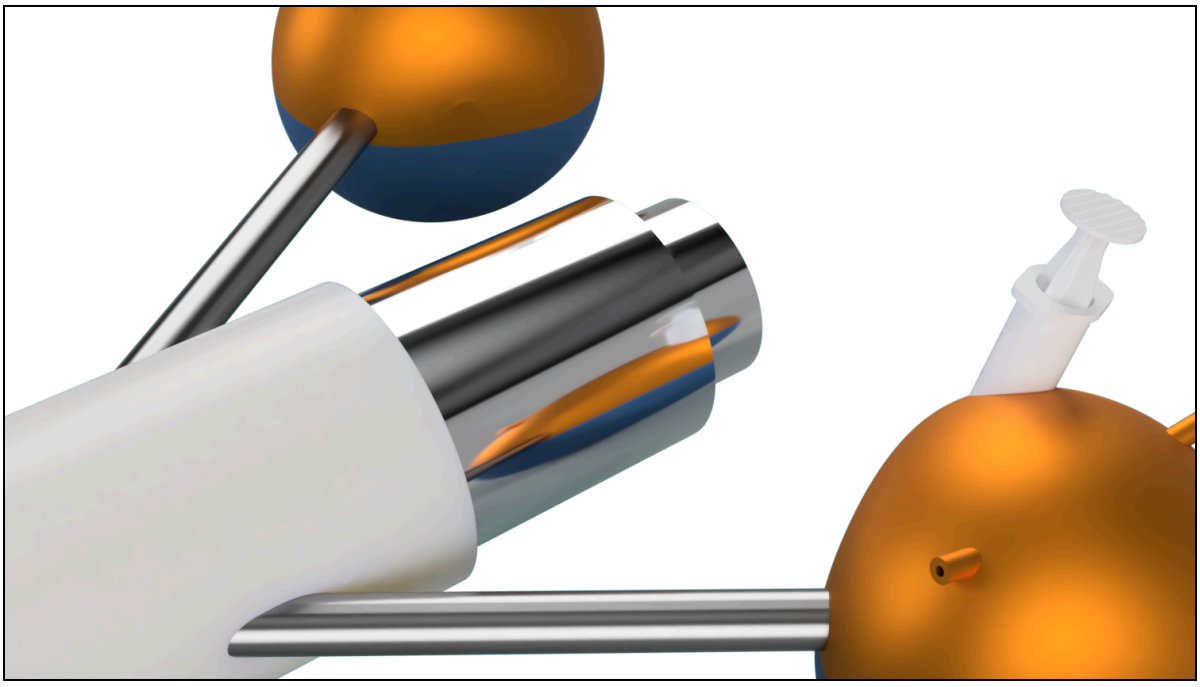

Figure 15: Combustion chamber design

Fuel Cell Research

One option for the fuel cell component of the project was to manufacture our own fuel cell. To do this, we decided to purchase membrane electrode assemblies and build a fuel cell using them. Membrane electrode assemblies (MEA) are the core component of a fuel cell that helps produce the electrochemical reaction needed to separate electrons. A schematic of the different layers of the MEA is shown in Figure 16 below. On the anode side of the MEA, a fuel (hydrogen, methanol, etc.) diffuses through the membrane and is met on the cathode end by an oxidant (oxygen or air) which bonds with the fuel and receives the electrons separated from the fuel. Catalysts on each side enable reactions, and the membrane allows protons to pass through while keeping the gases separate. In this way, cell potential is maintained, and current is drawn from the cell, producing electricity.[1]

A typical MEA comprises a Polymer Electrolyte Membrane (PEM), two catalyst layers, and two Gas Diffusion Layers (GDLs). Due to its composition, an MEA with this configuration is known as a 5-layer MEA. An alternative version of a membrane electrode assembly is the 3-Layer MEA, which is composed of a polymer electrolyte membrane with catalyst layers applied to both sides, the anode and cathode. An alternative name for this type of MEA is a Catalyst Coated Membrane (CCM).[1] These MEAs can also be constructed as reversible assemblies to be used in reversible fuel cells.

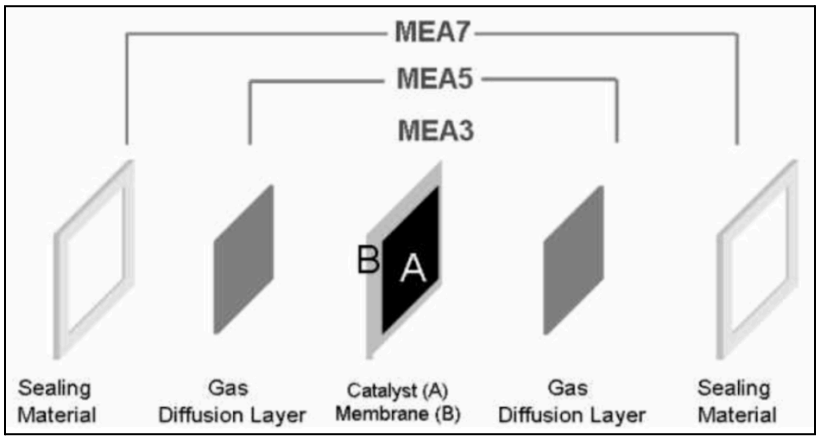

Figure 16: Schematic of Membrane Electrode Assemblies[1]

Ultimately, we decided not to construct our fuel cells because it would be too difficult to properly seal the MEA, and the assembly would be at risk of leaking hydrogen gas. As such, we purchased a fuel cell from the fuel cell store that implemented the reversible MEAs discussed previously. We bought a Double Reversible H2/O2 Fuel Cell from the fuel cell store, as shown in Figure 17 below.

Figure 17: Isometric view of the Double Reversible H_2/O_2 Fuel Cell[3]

The technical specifications for this fuel cell are listed below:

- Electrolyser Mode: 10 cm^3/min H_2; 5 cm^3/min O_2; 2.33 W
- Fuel Cell Mode (O_2): 1000 mW
- Fuel Cell Mode (Air): 400 mW
- H x W x D: 56 x 42 x 57 mm
- Weight: 63 g

A schematic for the experimental setup of this fuel cell when operating in the electrolysis mode (turning water into H_2 and O_2 gas) is shown in Figure 18 below.

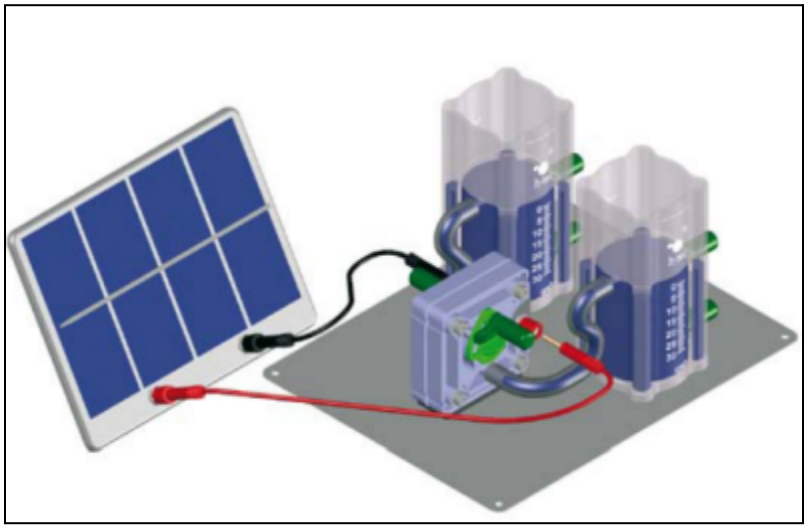

Figure 18: Experimental setup for electrolysis mode of the reversible fuel cell[3]

Experimental testing with this fuel cell proved that it was difficult to make the reverse process work (turning H2 and O2 gas back into water). This is because upon completion of the forward process, the membrane would be flooded with water, and the fuel cell would be clogged, not allowing the gas to reach the membrane and thus preventing the reverse process and the conversion of the gases back into water. Hence, while we were able to use this reversible fuel cell successfully in the electrolyzer mode to produce gases from water, we could not turn these gases back into water in the fuel cell mode using this same device. This problem was also noted by the previous research team that worked on this technology, Bay-Max. As suggested by Dr. Ghorbel, we decided not to focus on working around this problem, and we are instead settling on only using the fuel cells in the electrolysis mode. As such, we will use the BCDs only to achieve buoyancy control in the upward direction. Since buoyancy control using reversible fuel cell technology has already been proven possible both theoretically and experimentally (as was stated by work from the research group at the University of Houston), we decided we didn't need to spend more money on higher-quality reversible fuel cells that did not experience this problem.

Progress Compared to Goals

Goals set during Fall 2024

1. Determining the scope of the project

Our scope changed significantly from the initial plan. We wanted to create a robot that could swim, have buoyancy control, and jump. After our latest discussions with our advisors, this has been narrowed down to just upward buoyancy control for underwater “gliding” and combustion for jumping.

Actual result after Spring 2025

We succeeded in all of the above, being able to maneuver the robot buoyancy upwards, adjust rotation, and produce forward and upwards impulse while underwater. Our robot design is also capable of performing downwards rotation and downwards buoyancy control if reversible fuel cell technology could do them efficiently. In the interest of a high quality prototype, we went with the more efficient non-reversible electrolyzers.

2. Determine if gaseous hydrogen-oxygen combustion is viable for propulsion.

We researched various fuel propellants and concluded that gaseous H2 and O2 are a very viable reaction for propulsion. We learned through simulations that the ideal ratio is in fact, 2:1, to support maximum reaction. Even though there is no continuous thrust like in liquid propellants, this impulse reaction works as long as the concentration is adequate and no other gases are present.

Actual result after Spring 2025

We succeeded in using this fuel mixture with the above ratio to propel both a test vehicle on our test rail as well as our robot underwater, both directly forwards and forwards and upwards at an angle.

3. Make sure there is enough data from combustion to apply it to our robot

Recently, we have gathered successful data from testing the combustion. This allowed us to get rough velocity and acceleration plots. Now we are excited to know we are very close to having enough data to understand what is needed for the combustion chamber on our robot.

Actual result after Spring 2025

We have achieved clean position, velocity, and acceleration plots for our robot and have displayed them on our OEDK showcase poster.

4. 3DOF swimming

We began the project with the assumption that our BCDs would create the forward motion, but as the project progressed our scope redirected the forward propulsion to the combustion. Now we will still have 3DOF swimming, but it will be shared between the combustion and the BCDs.

Actual result after Spring 2025

Forward translational propulsion was achieved via combustion, and 3 degrees of rotation were achieved via BCDs.

5. If we have time, ensure the robot can glide in the air longer than acting as a projectile.

This goal began as a bonus to the work we were doing. We understood that this was just “icing on the cake”. As we continued to clarify the scope of our project, we realized that this goal is not likely to occur. This is just not needed for our project.

Actual result after Spring 2025

Upon discussion with Dr. Ghorbel, we mutually agreed to aim for underwater “gliding” instead, meaning that the robot would launch at an angle and change direction during the launch. This was indeed achieved.

6. Robot Design

Robot design has changed a lot throughout the semester. From gas reservoirs that control the flexing of tail ligaments via valves to silicone fishtails for swimming, we have tried many designs. Our current design that is shown in the CAD models above holds the most promise, as it is lightweight, considerate of combustion, and can house the microprocessor and all the electrolyzers.

Actual result after Spring 2025

We had a successful design and demo at the OEDK showcase, which featured videos showcasing its capabilities. Thus, the design was functional to our standards: it worked, was waterproof, and held the electronics safely and compactly.

7. Safety

We thoroughly wrote down our ideas for safe operation and submitted it to EHS. It was finally approved about a month and a half before the end of the Fall semester.

Actual result after Spring 2025

Upon approval, we immediately began testing at South Annex and followed all the necessary safety protocols.

8. Understanding the material given

Initially, we had very little knowledge about the parts needed to make the robot. But after lots of research and experimentation, we started understanding the individual mechanisms better and specialized in different robot aspects. We know a lot more than when we started, and we plan to put all the individual parts together during the spring.

Actual result after Spring 2025

We became very comfortable with the knowledge relating to waterproofing and the physics of combustion and electrolysis, as well as knowledge on how to make a remote control circuit for the BCDs. We ended up not having to design our custom fuel cell as it would get unnecessarily and prohibitively complicated (and error-prone).

System Engineering

As mentioned before, the need statement of our project is to design a soft-actuated, tetherless, lightweight, underwater robot capable of buoyancy control and propulsion via combustion reaction of H2 and O2 gas that is produced by reversible fuel cells. This is a sustainable robot, and theoretically, it has a long operating life if the gases and water are maintained in a closed-loop system, since there would be regenerative charging of the batteries. All of this makes our project ideal for exploring difficult-to-access areas for humans, such as wetlands, marshes, or other places with small puddles of water that our robot can jump into and out of. When equipped with the proper sensors, the robot can gather all sorts of data for various research projects.

In terms of need analysis, this research is crucial to further the development of soft robots because there is nothing out there that exactly meets our need statement. Most soft robots are tethered, and almost all of them use a fuel source that is either small batteries, pneumatic, or hydraulic power. These options are also generally environmentally friendly, but the combustion reaction of H2 and O2 gas (which is very energetic) can provide a strong impulse force similar to a jump, enabling our robot to have greater mobility compared to these other options. Our final robot is also relatively affordable and easy to produce. Costing just $500 (primarily due to the electrolyzers, which have rare earth metals inside for catalysts), the robot body is also entirely 3D printed, enabling researchers or hobbyists to print it themselves instead of relying on more expensive machinery for fabrication. Since our robot is soft-actuated, it does not depend on servos or motors for complex movements, which may have issues with breaking down.

With regards to functional decomposition, our final goal can be broken down into its constituent parts rather nicely. The final robot, is composed of four central systems: the combustion, buoyancy control, overall chassis, and electronics. It was necessary to design chamber prototypes with different shapes so that the thrust could be maximized. It also needs to fit the maximum amount of pure H2 and O2 gas mixture while starting from a vacuum. All of this was met one at a time, from making subsequent iterations and running tests each time on our

above-water test rig. From this, we put the footage into analysis software to determine velocity, acceleration, impulse, and force. For buoyancy control, we ran tests with different power sources, such as 9V batteries, battery banks for phones, and ideal power sources, to determine how much gas filled the balloons and at what rates. From this, we could have rough estimates of the operation. For the chassis, we had to CAD it and fix it each time the print did not work as expected or if the plans changed. For electronics, we had to listen to what each group wanted for controls, create it into a small electronic circuit, and then wirelessly control the Arduino from our laptops.

All of this is relevant to systems engineering because we are taking the entire system and seeing what needs to be done for each step of the way to get the final product. For example, the final specification of control for three directions of freedom is enabled by careful adjustment of the buoyancy control device, which we theorized for months and finally proved with our final aquatic tests. Our goal of determining if H2 and O2 gas combustion was a viable method for propulsion was also demonstrated once we had the tests on land in the test rig and underwater in the final chassis.

Safety Analysis

To ensure our underwater robot's safe development, testing, and potential deployment, we constructed a comprehensive Environmental Health and Safety (EHS) approach to our design work. Our safety considerations were guided by the Failure Mode and Effects Analysis (FMEA) methodology. Our robot utilizes electrolysis to produce gaseous hydrogen and oxygen, which are then combusted for propulsion. This functionality carries an immense safety risk that we identified and mitigated. The FMEA process informed our design choices for potential client or customer use to ensure we reduce the safety breaches.

Our safety procedures were developed in agreement with Rice University’s EHS policies. These procedures were also formally approved by the university’s EHS department and our faculty sponsors. Implementing these protocols was critical to reducing the likelihood of a potential hazard during testing. The FMEA shown in Table 4 outlines the key failure modes, effects, causes, risk severity, methods of mitigation, and whether the risk applies to the building or testing of the prototype or during use by someone outside the team. The level of severity ranges from 1-10, where one is the least severe and 10 is the most severe. The level of occurrence, “likelihood,” also varies from 1-10, where one is the least and 10 is the most. The level of detection is how likely one is to be aware of a failure mode taking place. This range 1 is the most likely to detect, while 10 reflects the most unlikely to detect. Finally, RPN represents the Risk Priority Number. This value helps discern which failure modes are the most important to prioritize.

Table 4: Failure Mode and Effects Analysis (FMEA)

Failure Mode	Effect	Cause	Severity	Likelihood	Detection	RPN	Mitigation Action	Applies to
Gas entering the robot's body	Can destroy electronics if combusted	Loose fittings or seal failure	10	2	8	160	Pre-test gas production, proper Teflon application	Testing
The spark plug does not fire	Operational Failure	Electrical short or poor wireless connection	8	3	4	96	Ensure proper connection of wiring. Visual power indicators	Testing and client use
Residual flame	Fire hazard after the test	Non-combusted hydrogen	7	2	5	70	Fire extinguisher and post-test inspection	Testing
One-way valve failure	Can destroy electronics if combusted	Excess combustion	10	2	7	140	Set an upper bound for max combustion runs	Testing
Environment disturbance	Habitat damage or contaminati on	Poor testing location	4	2	3	24	Select a non-sensitive site	Testing

* RPN = Severity x Likelihood x Detection

Since gaseous hydrogen and oxygen are the fuel and oxidizer used for our combustion, water vapor is the only byproduct. This means there are zero harmful environmental emissions. Therefore, the significant ecological risk we considered was for our testing location. We needed to ensure a place where ecological sensitivity was not of considerable concern. Consequently, we selected Rice's South Annex as the testing area due to the lack of ecological risk and clear surroundings.

The structured approach provided by the FMEA methodology allowed us to effectively identify hazards and mitigation techniques to ensure safe operation during our various building and test phases. With these concerns in mind, the team can further develop improved safety measures for the use of the underwater robot.

Testing Procedures

Linear Combustion

For initial linear combustion testing, we first had to prove the concept of fuel cell-driven combustion. To achieve this, we designed a linear combustion testing rig that could be utilized for repeatable testing. Its base consisted of two parallel linear rails with attached linear bearing sliding blocks. We developed and 3D printed a modular and scalable attachment that served to integrate the combustion chamber to the slider blocks, such that we could record the distance and time that the system slid across the rails. We also added an electronics and fuel cell housing box that easily screwed into our sliding blocks.

This test was designed to evaluate our fuel cells' capabilities of driving combustion through electrolysis and the production of hydrogen and oxygen gas. It also assessed the performance of different combustion chamber designs. The requirements would be met if the combustion reaction produced any type of observable movement in our sliding system. From there, an analysis of a visual recording of the motion would be used to gauge the relative performance of the chamber.

Throughout this design project, multiple chambers composed of different materials and fabricated with varying methods were tested. Additionally, other periods of gas production were tested to determine how the performance of the different chamber designs changed with the amount of gas stored in the chamber.

1. Collect and assemble all essential components for combustion testing
    - PEM fuel cell
    - Wires
    - Elastic tubing
    - Battery/power source
    - Spark plug
    - Combustion Chamber
    - Syringe
    - Distilled water
    - Pressure vessel to contain the explosion
    - Rails
    - Sensors
2. Ensure the spark plug is not connected to power
3. Turn on the fuel cell and observe the production of gas
4. Check plumbing connections and ensure there are no leaks
5. Turn off the fuel cell and release gas within the pressure vessel
6. Stand approximately 35 feet away from the test setup
7. Connect the spark plug to the power
8. Turn on the fuel cell and wait till the predetermined amount of fuel is produced.

9. Turn off fuel cells
10. Ignite the spark plug, propelling the device across horizontal guide rails
11. Wait for the device to stop
12. Disconnect the spark plug from the power and ground the system
13. Spray a carbon dioxide fire extinguisher over the site to extinguish difficult-to-see flames
14. Inspect the test setup for any significant damage

Waterproof Testing

1. Collect and assemble all essential components for waterproof testing
    - PEM fuel cell
    - Wires
    - Elastic tubing
    - Battery/power source
    - Spark plug
    - Combustion chamber
    - Syringe
    - Distilled water
    - Water bucket
2. Turn on the fuel cell and observe the production of gas
3. Check plumbing connections and ensure there are no visible leaks
4. Submerge the chamber in water, and observe any bubbling from leaks in the chamber

This test was done many times throughout our design as we iterated on our combustion chamber setup. With that, we based our requirements on whether the combustion chamber met our requirements of being completely waterproof on visual observation or lack thereof, bubbling while underwater, and during electrolysis for gas to be produced.

BCD and Robot Buoyancy

Buoyancy testing for the BCD and the whole robot was conducted in similar ways. The BCD buoyancy testing was done in a bucket, while the much larger Robot was tested in a fish tank. This testing was done to ensure neutral buoyancy of the BCDs first, and then the Robot as a whole. Neutral buoyancy is essential to ensure that the robot does not float uncontrollably without us activating the BCDs. Buoyancy testing of the BCDs and the robot was conducted using the following steps.

1. Measure the total volume of the BCD/robot using CAD Fusion software
2. Measure the total mass of the BCD/robot physical prototypes using a scale
3. Calculate density using measured mass and volume values
4. Add weight to BCD/robot as needed to ensure the density is equal to or greater than 1000 kg/m^3
5. Manufacture necessary weights equal to what was determined in the previous step using a 1-inch-thick solid steel bar and insert them into the BCD/Robot

CFD Analysis

The software SimScale was selected to conduct the CFD analysis. The CAD model was modified to include an external fluid enclosure surrounding the robot's geometry. The newly designed enclosure was included in the simulation, and objects from the original imported CAD files were excluded to isolate fluid interactions with the primary body. It is also important to note that the surface of the robot was simplified to a geometry that did not include the complex surface finishes of the real robot. This simplification, like an Ahmed body, will reduce computational time while also providing an analysis of the hydrodynamic performance within a reasonable estimate.

The simulation assumed one-dimensional motion of the object at a constant velocity of 1 m/s. The freestream velocity of the fluid was also set to 1 m/s to eliminate relative motion between the object and the surrounding water. This simplification removes boundary layer effects from the analysis, allowing for more direct analysis of flow behavior around the robot. The simulation domain had a depth of 1 meter to capture relevant hydrostatic pressure influences, similar to what we would see during testing. Water was used as the working fluid, and it was modeled as incompressible due to the low velocity of the analysis.

The lift direction was defined as the y-axis (perpendicular to the inlet velocity), and drag was measured along the x-axis (parallel to the inlet flow). The projected frontal area of the shell was used as the reference area for force calculations. The reference length, defined as the characteristic dimension perpendicular to flow direction, was measured within the software. While the center of rotation was not emphasized in this study, it will become increasingly important in future simulations involving more complex movement within deep waters.

Mesh generation was performed with a region refinement of a maximum edge length of 0.02 m. Additional refinements were applied to the wake region using a Cartesian box created through primitive geometry. Custom surface refinements were used on the robot's faces by applying a minimum element size of 0.006 meters. Mesh quality was verified before running the simulation. The CFD simulation provides a velocity magnitude contour of a body subjected to fluid flow in a two-dimensional, top-down configuration. The flow direction is from left to right, with a maximum recorded velocity of approximately 1.25 m/s.

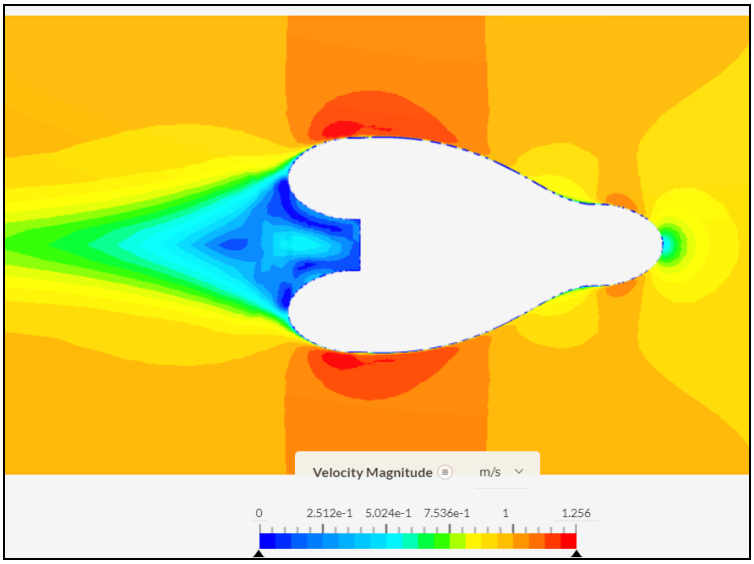

Figure 19: Top View: Fluid Flow Velocity Field

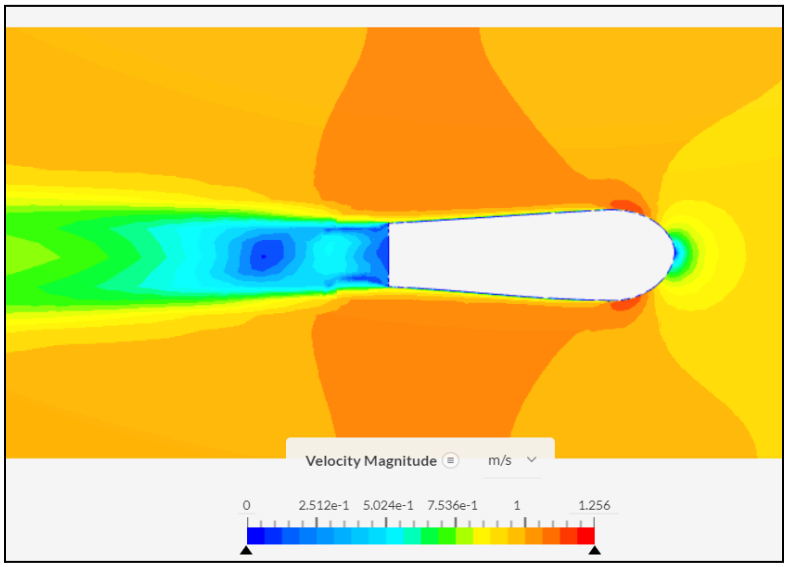

Figure 20: Side View: Fluid Flow Velocity Field

Figures 19 and 20 present a top view and side view of the velocity field around the body, respectively. The incoming fluid enters at 1 m/s, and the flow topology indicates the formation of vortices on the rear of the robot body. Near the front of the body, a stagnation region is visible, where the fluid decelerates immensely by contacting the leading surface. This is consistent with theoretical expectations, as the incoming fluid encounters resistance from the front geometry, resulting in near-zero velocities at the stagnation point. This is visually displayed by the dark blue dot at the front of the robot.

As the fluid moves along the curved surfaces of the body, it accelerates around the top and bottom contours, reaching higher velocities as indicated by the red and yellow colors. These changes in velocity suggest that the object exhibits airfoil-like behavior, where the geometry provides streamlined flow over the body. The higher speeds observed at the top and bottom curves of the robot reflect a geometric symmetry. This is essential to reducing any imbalances during the robot's operation. In contrast, the rear portion of the body shows a large wake region where fluid velocity significantly decreases. This forms clusters of vertices and zones of separation. These are represented by the cooler blue and green shades trailing the object. The separation in this area indicates a breakdown in laminar flow and the generation of turbulence, which leads to increased pressure drag. The lack of smooth tapering at the end likely contributes to this flow detachment, preventing pressure recovery and a continuous, streamlined flow.

The simulation results reflect that while the object's forward geometry encourages smooth flow and minimizes initial drag, the trailing edge could be improved through design modifications. Potential improvements include tapering the rear geometry to reduce wake formation. Such a refinement would improve the overall hydrodynamic performance of the system, especially during forward propulsion through water.

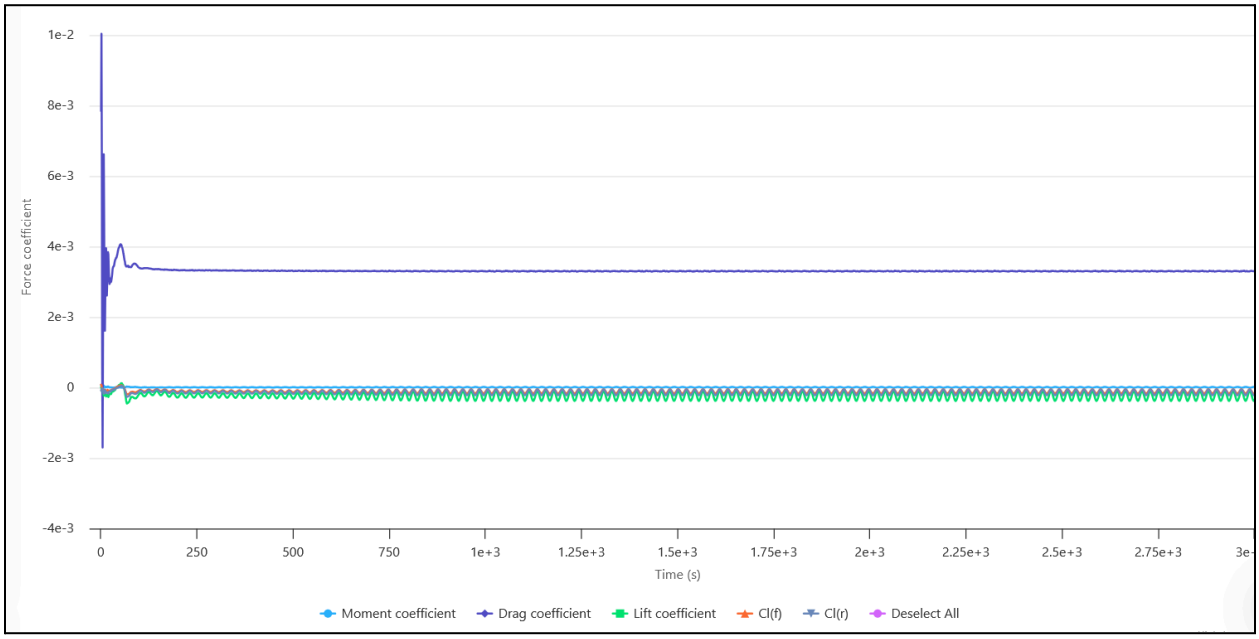

Figure 21: Force and Moment Coefficients Plot

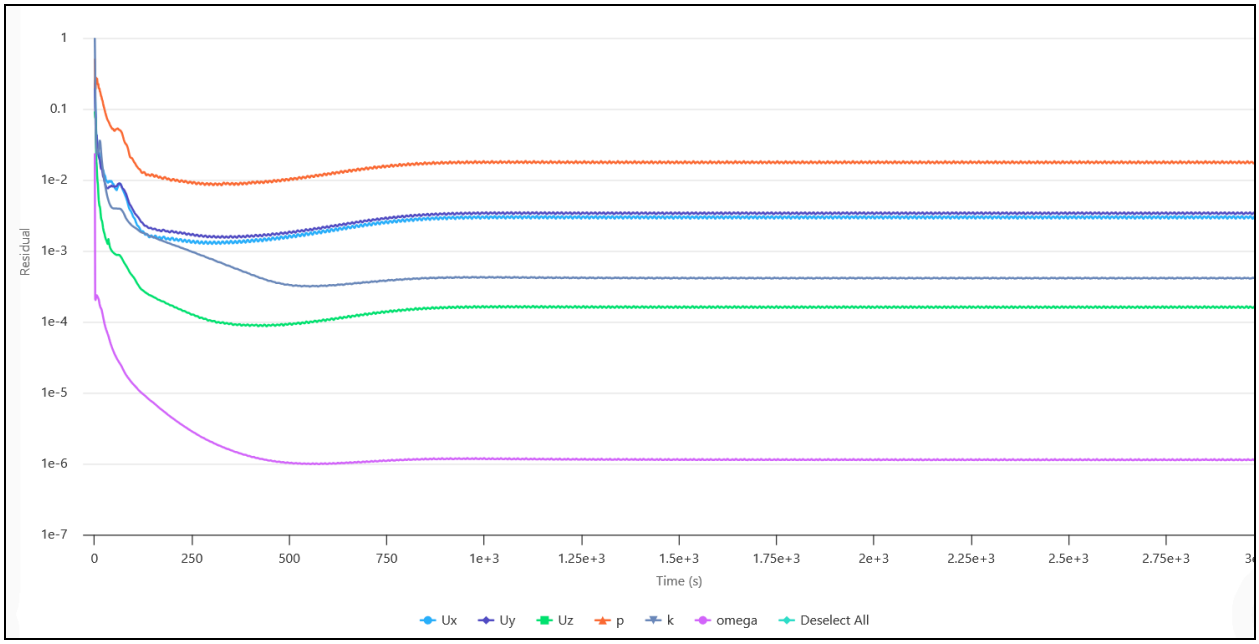

Figure 22: Residuals Plot

Next, the computational performance of the simulation can be analyzed. Force and moment coefficients, shown in Figure 21, converged in about 900 seconds of the 3000-second simulation. This convergence indicates that the simulation was well-defined and efficient in solving the governing equations for an in-depth model. Residual plots in Figure 22 further confirm the accuracy of the solution. The velocity residuals Ux and Uy reached magnitudes of $1x10^{-2.5}$, and the residual for Uz converged to a value of $1x10^{-3.8}$, demonstrating a low error margin across the domain. Although residuals for pressure and turbulent kinetic energy (k) were not as low, they remained within acceptable limits. The specific dissipation rate (omega) residual achieved a value as low as $1×10^{-6}$, indicating highly accurate resolution of turbulence characteristics. Local mesh refinements could further improve the convergence of pressure and turbulence residuals in future runs.

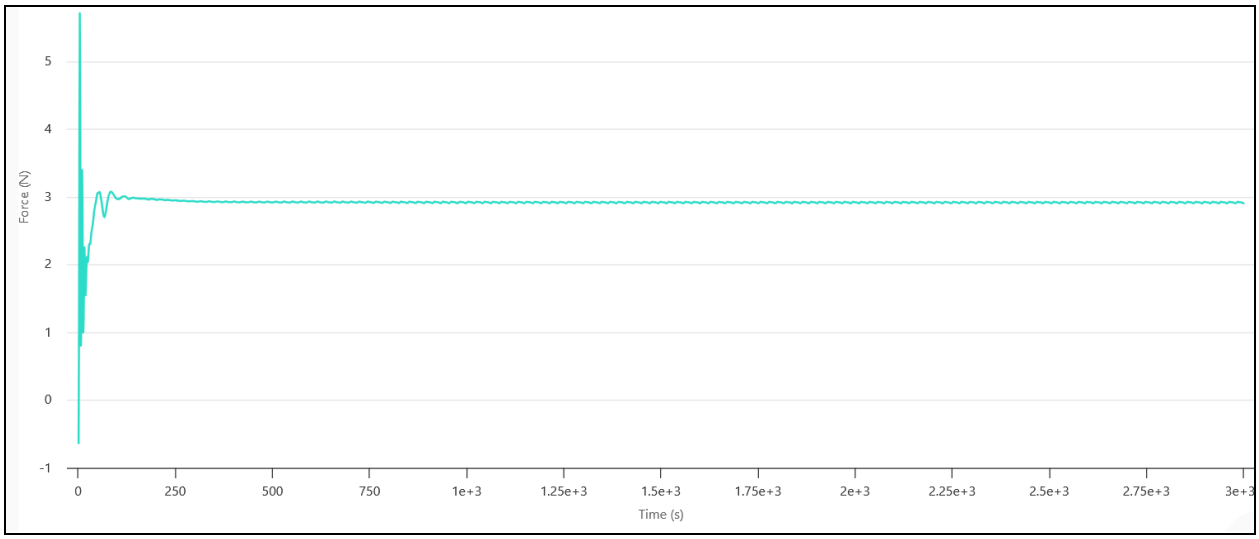

Figure 23: Total Force in X-Direction Plot

Figure 23 displays the total force in the x-direction (3N), which was used to compute the drag coefficient using the standard drag equation:

$$F_D = 0.5 * \rho * v^2 * C_D * A$$

From the simulated force, the drag coefficient of the entire robot was calculated to be 0.244. This value falls between the aerodynamic efficiency of a streamlined airfoil (typically around 0.05) and that of commercial vehicles (typically between 0.25 and 0.3). The result suggests that the robot body demonstrates promising hydrodynamic performance and supports the viability of the design for underwater movement.

Integrated Test

The following testing procedure ensures we are able to observe and collect data on the two functionalities of the robot (buoyancy control and propulsion) as well as the overall performance of the remote controls. Similar to on-land testing, we followed various safety protocols to ensure the team minimized any potential hazards.

1. Collect and assemble all essential components for fully integrated testing
    - Pill
    - Complete BCDs (3)
    - 9V Batteries
    - Power Banks
    - Wires
    - Elastic tubing
    - Spark plug
    - Combustion Chamber
    - Distilled water
2. Ensure the chamber is completely rid of all hydrogen and oxygen gases from the electrolyzer.
3. Test the spark plug before gas production
4. Ground the system and cut power to the spark plug
5. Check that the electrolyzers inside the BCDs work individually and effectively inflate the respective balloons.
6. Turn on the combustion chamber electrolyzer and observe gas production in the chamber.
7. Check plumbing connections and ensure there are no leaks
8. Reconnect the spark plug
9. Submerge the whole robot in water
10. Wait a few minutes to ensure there are no leaks in the system
11. Turn on electrolysis in one of the BCDs to observe the robot's rotational capabilities
12. Turn off the electrolysis in the BCDs
13. Ensure the chamber plunger is in contact with a heavy object (brick).
14. Turn on electrolysis to produce hydrogen and oxygen gas for 3 minutes
15. Turn off the electrolysis in the chamber
16. Ensure that the involved parties are 35 feet away from the testing setup
17. Turn on the spark plug and record the test

Final State of the Project (Spring 2025)

Overview of Final Design

The final design of the MUDKIP robot is shown in Figure 24 below. Figure 24a shows a CAD rendering of the final design that was created using Fusion. This rendering includes every part of the robot, including the pill, BCDs, combustion chamber, balloons, and lid. Figure 24b shows a photograph of the final prototype of the physical robot. This image shows the entire robot in the final state in which it was tested for our final results section. All of the BCDs are attached to the pill using screws, the combustion chamber is permanently affixed to the pill, all of the electronic components are in the pill, and the lid is screwed on with teflon for a secure seal. The colors for this robot (orange and blue) were chosen both to reflect our team's mascot, the Pokémon Mudkip, and for visibility in water. The balloon colors were also selected for this purpose, in addition to helping differentiate between the hydrogen gas (orange balloon)and oxygen gas (blue balloon), which needed to be kept separated in the BCDs to avoid unwanted combustion. This final robot design is waterproof, wirelessly controllable, equipped with complete orientation control via BCDs, and exhibits controllable working hydrogen-oxygen combustion for forward propulsion. Each of these different components of the robot will be discussed in significant in-depth detail in the following sections of this chapter.

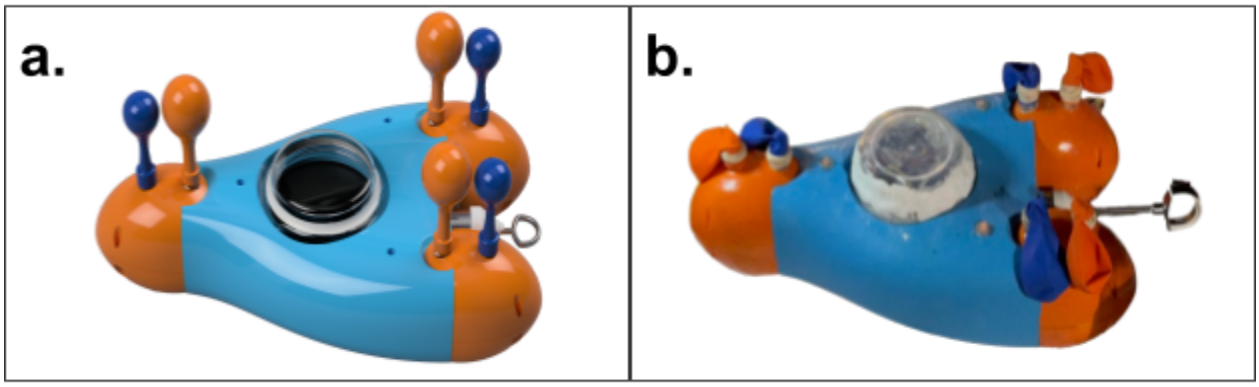

Figure 24: a. CAD render of final robot design. b. Physical prototype of the final robot design.

The final design of the Buoyancy Control Device (BCD) is shown in Figure 25 below. Figure 25a shows a CAD rendering of the final BCD design. This includes the balloons, joint for pill attachment, screws, and both the top and bottom shell halves. Figure 25b shows a photograph of the physical prototype of the final BCD design. This photograph shows a complete BCD with all the internal components, including the electrolyzer, tubing, DI water chamber, and added weights. This final BCD design is compact, hydrodynamic, waterproof, and has been proven effective experimentally. Once powered using an external power supply, with the electrolyzer on and producing gas, the BCD takes approximately 1 minute to move from a neutrally buoyant state to a floating state. An in-depth and detailed discussion of the design of the BCD can be found later in a section of this chapter.

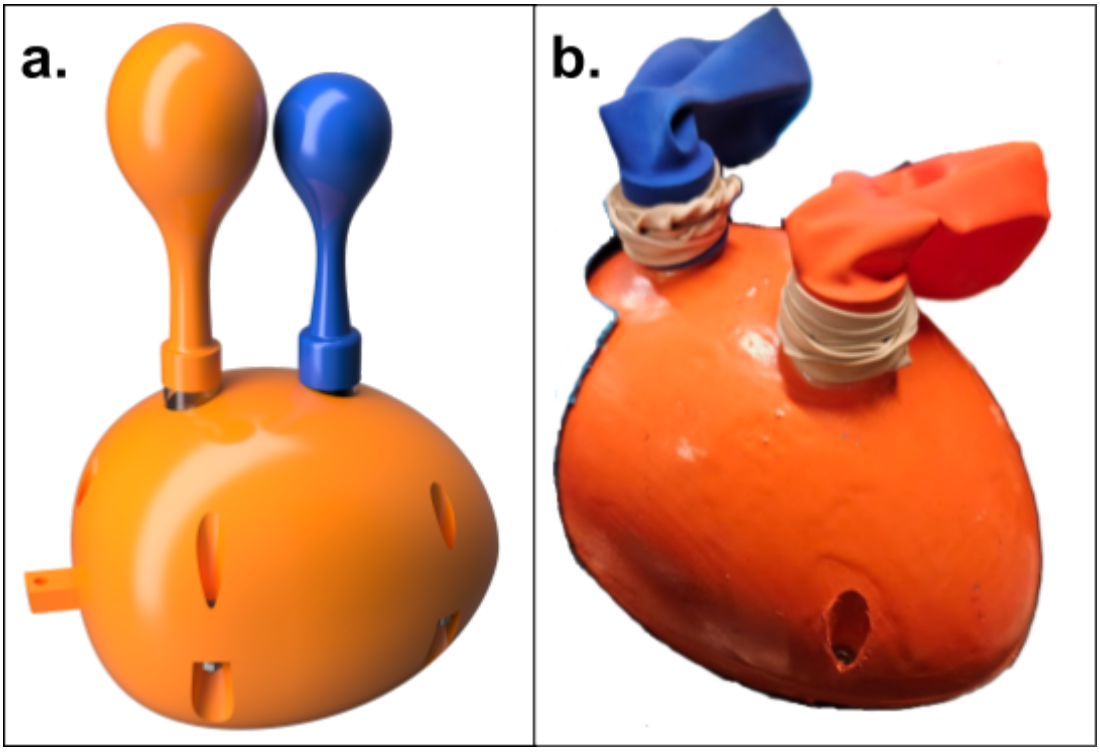

Figure 25: a. CAD render of final BCD design. b. Physical prototype of the final BCD design.

A CAD rendering of the final design for the combustion chamber used for forward propulsion in this robot is shown in Figure 26 below. This combustion chamber is composed of several parts, including the plunger with O-Ring, end cap, check valve, and the bung for spark plug attachment. After several design iterations and experimental trials, this combustion chamber design was optimized for the best performance in single-use hydrogen-oxygen combustion for forward propulsion that this team could achieve. While this particular design is only viable for single-use combustion, some alterations can be made to it that would allow for repeatable combustion, such as the incorporation of a high flow rate check valve instead of the plunger. More information on the combustion chamber, its use in forward propulsion for the robot, and its attachment to the pill can be found in the later sections of this chapter.

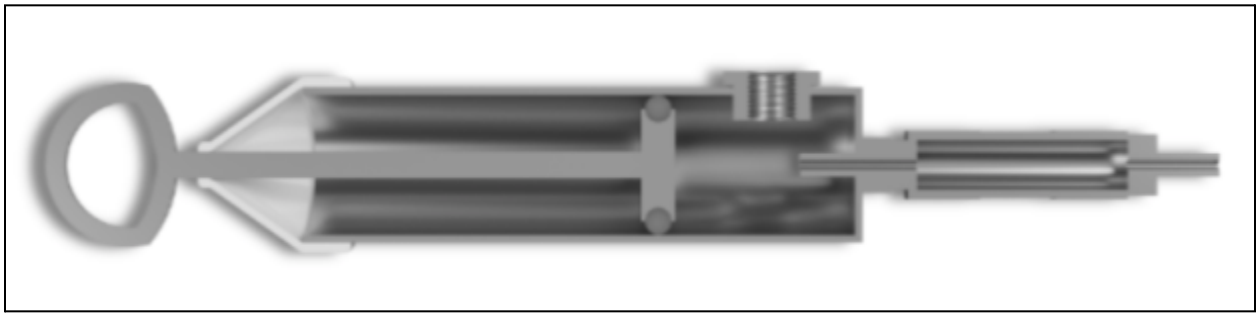

Figure 26: CAD render of final combustion chamber design.

Electronics

The electronics were minimized in size and stored neatly inside the “Pill” chamber of the robot. The Arduino is the central processing unit for the robot, and it receives signals sent wirelessly from a control station (laptop) before being used to control gas production in the electrolyzers that fuel the three BCDs and the combustion chamber. This wireless communication was achieved via a 2.4GHz wifi hotspot to which both the Arduino and control station were connected.

The Arduino uses GPIO pins in on/off states to toggle gas production on the electrolyzers. Our circuit features a MOSFET transistor, which, when grounded to the Arduino, allows the GPIO pins to toggle on/off the connection between the negative pin of the electrolyzer and ground. With the electrolyzer positive and connected to the power bank positive terminal, closing the electrolyzer negative-ground gap means there is current passing through the electrolyzer and turning it on. The second MOSFET (the “short” MOSFET) is turned on very briefly before each electrolyzer is toggled on, and then is toggled off. Its purpose is to create an almost-zero resistance pathway to facilitate charge flow from the power bank, as the power bank would not turn on at high resistances (from a current draw that is too low). Once the power bank is on, we turn off this pathway to funnel the charge into the electrolyzer. We do this as a way to automatically turn on the power bank, whose power-saving feature automatically turns it off after a period of disuse.

To ensure that our circuit actually works, we connected some GPIO read pins to the output of the power bank, which gives the user feedback in the laptop terminal on whether the power bank was successfully turned on, or if one has turned off. This lets the user know whether the system is functioning as intended or if the power bank needs to be restarted.

Our circuit design is very modular, with one electrolyzer utilizing two MOSFETs, and one power bank powering two electrolyzers. The connection is also modular and straightforward, with the positive terminal of the electrolyzer going to power and the negative going to the MOSFET drain. The MOSFET source is connected to ground, and when the MOSFET is on, the source and drain are connected.

We also feature a singular MOSFET for detonation of the combustion chamber gas. The signal is also sent via GPIO and toggles the same negative terminal-ground connection, but for a high-voltage transformer circuit board, whose positive input is wired to the Arduino’s 5V output and a flyback diode to prevent current backflow that could damage the transformer or Arduino. The transformer circuit contains a transformer coil and capacitors that store charges for spark production and circuit protection. The circuit board amplifies the voltage to kilovolts to create a spark. This output is wired to a spark plug, which is securely fastened to the combustion chamber. The positive output goes to the electrode, and the negative output goes to the entire chamber, which is electrically connected to the ground of the spark plug. Finally, the connections are then insulated and leak-proofed with various tapes for safety against electricity, water, and gas leaks.

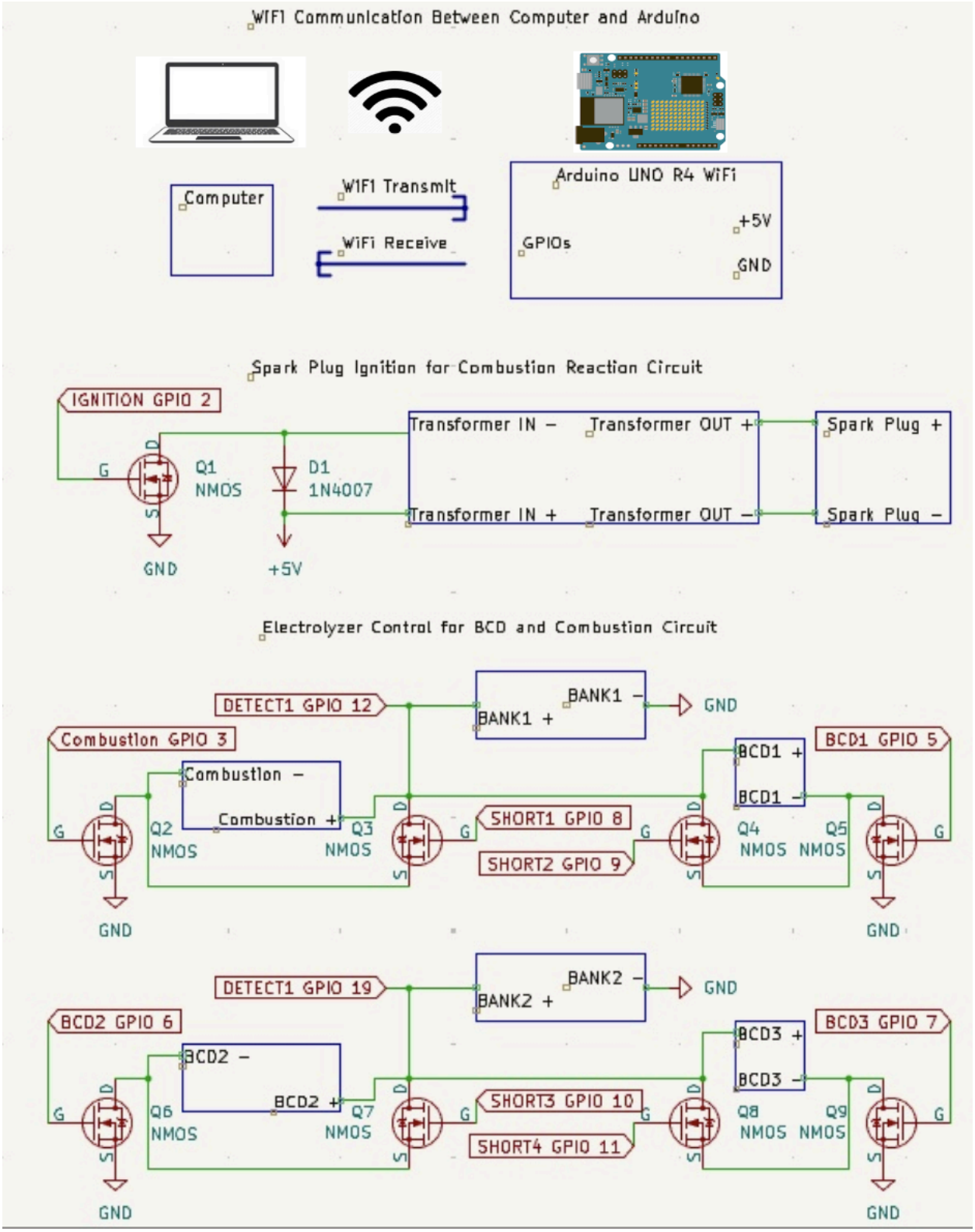

Figure 27: Final schematic for ignition control and electrolyzer controls with 2.4 GHz WiFi transceiver

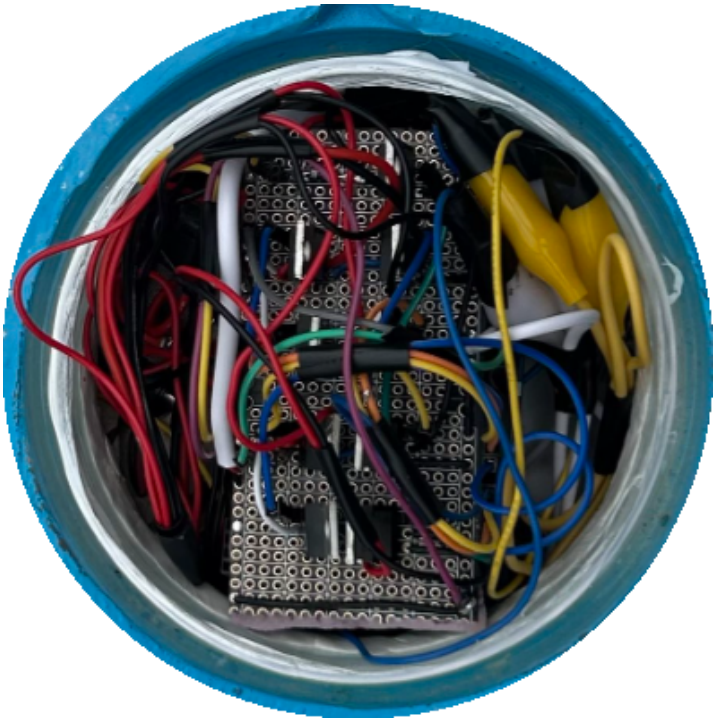

Figure 28: Interior of the pill once electronics are completely fitted inside. All the waterproofing is completely shown.

Combustion

For the final design, a stainless steel meat injector syringe was used as the base of the chamber. A washer of the same material was welded to one end of the injector, and a NPT fitting was then welded onto the washer. A check valve was screwed onto the fitting with a layer of teflon tape in between to ensure a good seal. The valve allows the hydrogen and oxygen gases produced by the electrolyzer to flow into the chamber, but stops backflow caused by the increased pressure during combustion. The other side of the chamber has the syringe plunger and a customized PLA cap to hold the plunger concentric with the chamber. This ensures that the force produced by the plunger popping out of the chamber is linear, mainly in the direction of motion, thus not losing any of the thrust produced. Lastly, a drill press was used to create a hole in the upper section of the chamber perpendicular to the cylinder, and a bung fitting (for the sparkplug) was inserted and welded into the hole.

The current capabilities of this combustion chamber are a single-use combustion reaction with a maximum of 90 mL of gas produced within 3 minutes of gas production from a single electrolyzer. It is powered by a standard household power bank, and it produces 21 N of thrust. It is completely leak-proof and has been completely submerged in water for a total of more than 5 hours. Additionally, it is designed to be modular so that the plunger, PLA cap, and check valve can all be removed and replaced if necessary. Additionally, given the capabilities of the chamber, it could be set up with different electrolyzers and still work as intended.

Our main struggle with the design was leaks caused by the welds. Although the metals used were all made of stainless steel 304, poor welding created multiple leak points along the washer and the bung fitting. To fix this issue, we applied generous underwater JB weld to the welded joints. We conducted waterproof testing after each application to determine the effectiveness of the JB weld. Eventually, we obtained a completely waterproof design.

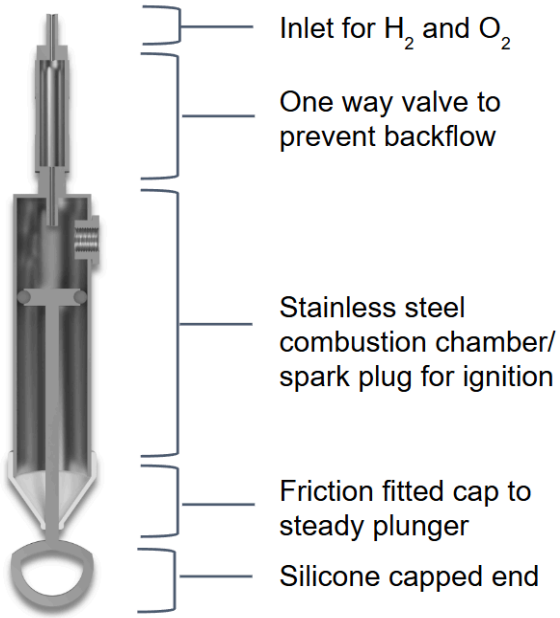

Figure 29: Combustion Chamber Cross Section

BCD Design

Buoyancy Control Devices (BCDs) are the methods with which the depth and orientation of this robot will be controlled. Each BCD will be able to maintain its buoyancy by changing its density using a mechanism that inflates/deflates balloons on the device. Inflating the balloons will increase the volume, reduce the density, and increase the buoyancy force on the device, thus moving the BCD up in water. Deflating the balloons will reduce the volume, increase the density, and decrease the buoyancy force on the device, thus moving the BCD down in water.

The primary method with which the inflation/deflation of the balloons will be controlled is to use three options: Electrolyzers, PEM Fuel Cells, and Reversible Fuel Cells. Electrolyzers take an input of electricity and Deionized (DI) water and output Hydrogen Gas (H2) and Oxygen Gas (O2), thus allowing for balloon inflation. PEM (Proton Exchange Membrane) Fuel Cells take an input of H2 and O2 gas and output electricity and DI water, thus allowing for deflation

control. Theoretically, Reversible Fuel Cells can provide the functions of both Electrolyzers and PEM Fuel Cells, thus allowing for both inflation and deflation control. Experimentally, however, our team determined that the forward mode (Gas->DI Water) of the reversible fuel cell was difficult to properly integrate due to water saturation problems on the fuel cell membrane, resulting in extremely slow DI water production in the forward mode and less efficient Gas production in the reverse mode. As such, for this robot's demonstration, it was decided that electrolyzers were the best option, as they provided the most efficient gas production. Furthermore, inflation control is the primary objective of this robot's experimental demonstration, as our sponsor, Dr. Ghorbel, suggested.

The concept of the BCD itself (a device that controls its buoyancy in water using fuel cells) had already been proven viable by previous engineering design teams, such as the previous Rice University Team, BAYMAX, and our collaborators at the University of Houston. Their devices, however, were bulky, cumbersome, and slow. As such, our goal was to optimize the design of a new device that would be smaller, more hydrodynamic, and faster at inflating the balloons. After a significant amount of time and several design iterations, the isometric view shown in Figure 30 below is the final version of our team's new BCD. This device is not only much more compact than previous designs, but it also demonstrates effective waterproofing, easy connection to the robot's main body, modularity for different types of fuel cells, relatively fast balloon inflation, and optimized hydrodynamics.

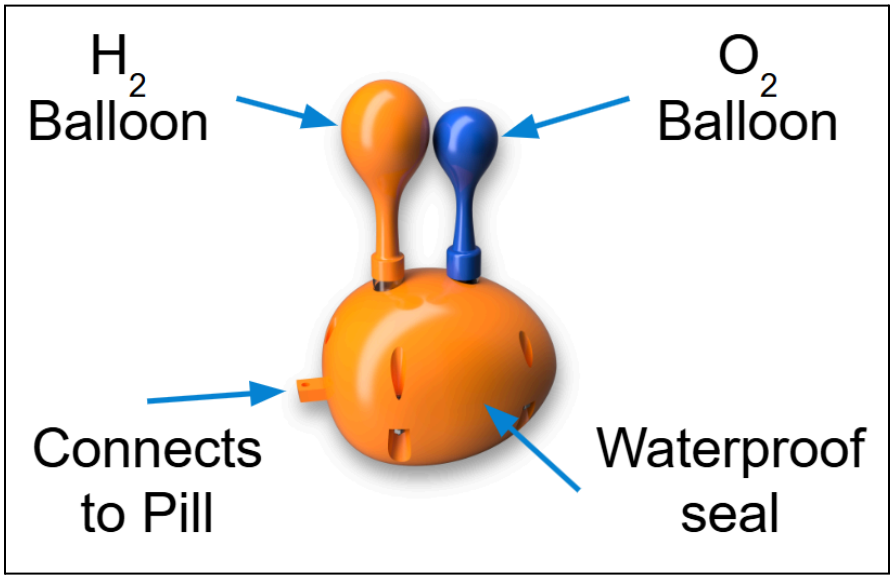

Figure 30: Isometric CAD render of BCD

The BCD has several intricate components and mechanisms (see Figure 31 below). All of the internal components of the device (balloons, electrolyzers/fuel cells, water syringes, and tubes) snap-fit into their proper locations. No fasteners hold the components together. The BCD consists of two outer shells (a top shell and a bottom shell) that are fastened together using 5 M3x0.5x18mm Stainless Steel Socket head screws. These two shells are manufactured from PLA using Bambu Lab X1C 3D printers.

The BCD's internal components are connected via 3mm ID x 5mm OD flexible pure silicone rubber tubing. At this size, the tubes fit tightly around all required elements The flexible material for this tubing was chosen in order to minimize kinks throughout the system. The inside of the BCD's top shell is also hollow, allowing space for slack tubing and preventing tubes from kinking. As such, these tubes ensure that DI water, hydrogen gas, and oxygen gas can flow through the system without leaks or interruptions.

Two separate balloons house gas in the BCD: the hydrogen balloon, shown in orange, and the oxygen balloon, shown in blue. These balloons are attached to the bottom halves of syringes using rubber bands. These syringes are then permanently affixed to the BCD's top shell using friction fitting and cyanoacrylate (super glue) and connected through the other side of the shell to the electrolyzer via silicone tubing. Hydrogen and oxygen must be kept in separate balloons because their mixture is combustible and dangerous. In these renders, the H2 balloon is much more inflated than the O2 balloon. This inflation difference is because electrolyzers and reversible fuel cells produce hydrogen gas at twice the rate of oxygen gas, per the chemical reaction and process outlined in the PEM Fuel Cell chapter. Thus, the difference in the balloon sizes in this render represents this difference in gas production rate.

In order to ensure that the BCD is neutrally buoyant when it is initially placed in water (with no inflation of the balloons), an added weight of approximately 40 g, manufactured using a stainless steel bar, is inserted into the BCD. This mass prevents the BCD from floating to the top of the water, as without the weight, the initial density of the entire BCD is less than that of water.

The water syringe holds deionized (DI) water for injection into the electrolyzer. To meet compactness, the syringe plunger is shortened, and a string is attached to its end to allow refilling with DI water while minimizing the syringe's extended length. For the BCD to function appropriately, the electrolyzer must first be primed by manually pushing DI water into the membrane. When electricity is supplied to the electrolyzer and primed with DI water, it will begin to produce H2 and O2 gas. Since the O2 gas is produced and outputted on the same side as the DI water is inputted into the electrolyzer (see Figure 2 in the PEM Fuel Cell chapter), initially, O2 gas will backflow into the water chamber. This backflow will cause the syringe plunger to be pushed upwards until it runs into a mechanical stop installed on the inside of the top shell of the BCD, right above the syringe. O2 gas will then build up in the syringe until the pressure equalizes, and the oxygen gas begins to flow into the balloon and inflate it. Once this process is complete, the hydrogen and oxygen balloons will inflate at a constant rate when the electrolyzer is supplied with electricity.

In order to supply the electrolyzer with electricity, two wires (one for the positive terminal of the electrolyzer and one for the negative terminal) are soldered to the electrodes of the electrolyzer. These wires are inserted through a hole in the back of the BCD's bottom shell. The wire hole is filled with layers of epoxy resin, cyanoacrylate (super glue), and J B Weld WaterWeld Epoxy Putty to ensure waterproofness at this possible leakage point. All materials

were added once they were fully cured to prevent shrinkage that can open micro-cracks on the surface.

Waterproofing is a significant area of concern for the entire BCD. The shells are 3D-printed at 100% infill to reduce water permeating through the outer surface of the BCD. This print setting also helps reach density requirements. On top of this, a thick layer of Smooth-On XTC-3D (an epoxy coating) is applied to the entire exterior surface of the shells to fill in any gaps and pores that may have occurred during printing. A double O-ring setup prevents water from entering the interface of the two Shells. Two O-rings of different inner diameters but the same cross-sectional diameter or width (Inner O-ring: Buna-N, 2-152. Outer O-ring: Silicone, 2-153) are placed into an O-ring groove designed according to the Parker O-ring Handbook specifications. The inner surfaces of the shells are sanded to provide a smooth interaction between the 3D-printed material and the O-ring. The two shells are then compressed using a significant amount of force by torquing five M3 × 0.5 × 18 mm stainless-steel socket-head screws to connect the shells. As stated before, the wire hole in the bottom shell of the BCD is waterproofed by filling it with layers of epoxy resin, cyanoacrylate (super glue), and J B Weld WaterWeld Epoxy Putty.

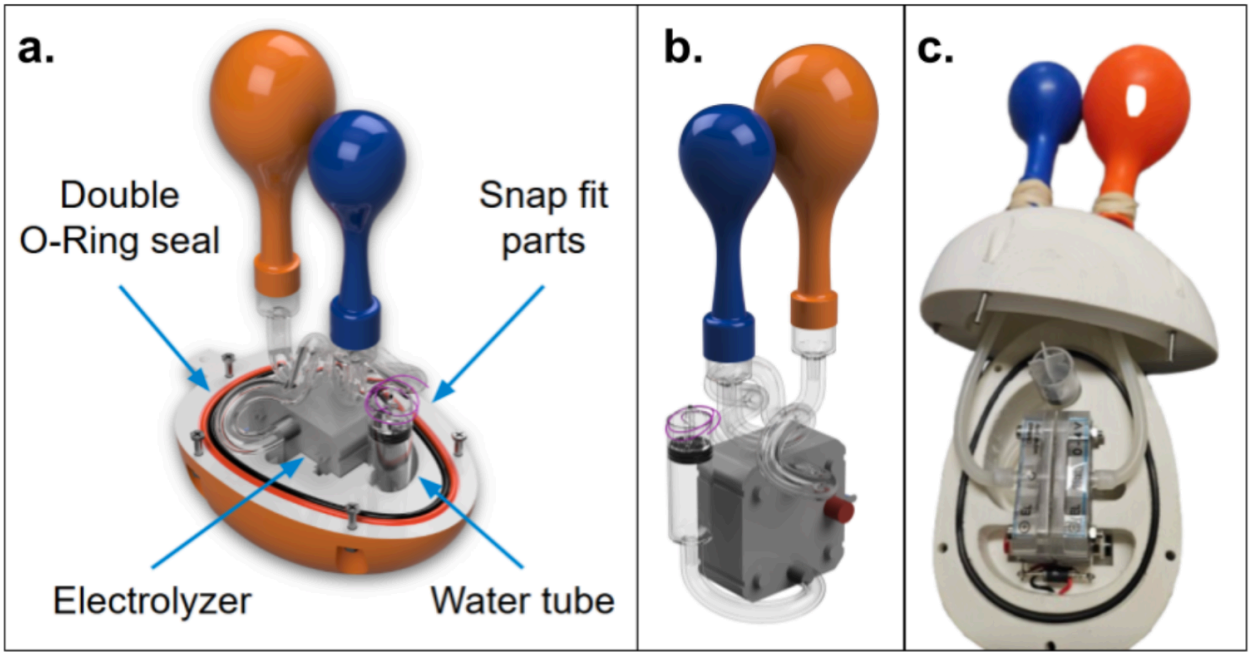

Figure 31: a. Isometric cross-sectional CAD render of the BCD with the Bottom Shell, Double O-ring seal, snap-fitted parts, electrolyzer, water tube, and balloons. b. CAD render of just the internal components of the BCD without the Bottom or Top outer shells. c. Cross-sectional view of the physical device prototype after it was assembled with all internal components.

The entire BCD is designed with modularity in mind. The BCD is easy to remove and attach to the main body of the robot using an extended piece on the back of the bottom shell that is inserted into a slot in the robot body. The BCD is then secured in place using one M3 × 0.5 × 18 mm stainless-steel socket-head screw that is inserted through the extended piece and

screwed into a nut inserted into a slot on the robot body. There is also slack on the wire that connects the BCD to the robot body, so that when the BCD is removed, it can be opened without needing to cut the wire connection. This wire slack has a specific groove in the robot body where it can be stored. If, in any case, the wire does need to be cut, it can easily be soldered back together with added heat shrink tubing and epoxy to ensure the wicablesre still waterproof. The BCD is designed to be modular and replaceable. It's only connected to the Pill through one pair of wires and mounted to the Pill using one M3 × 0.5 × 18 mm stainless-steel socket-head screw. The opening of the Pill has a 3D surface that matches the 3D surface of the BCD for a seamless fit. The BCD is mounted to the Pill by having an extension on the Bottom Shell that fits into an opening in the Pill. The corresponding slot in the Pill for the extension has an insert for a nut that secures the M3 screw.

Pill Design

The main robot body (referred to as the “pill” throughout this report) is the primary frame within which the BCDs, electronic components (such as the wires and Arduino), combustion chamber, and ignition system are held. The design of the pill was optimized in CAD to maximize hydrodynamics and interior space for electronic components. Unlike the previous team’s (BAYMAX) main robot frame design, our pill incorporates only 3 BCDs as opposed to 4. This is an intentional choice to help optimize hydrodynamics while maintaining the same degrees of freedom. While the previous team had one BCD on each corner of the robot, our design has one BCD in the front and two in the back. This allows the robot to narrow as you approach the front, making it significantly more hydrodynamic (as discussed in the CFD Simulation section of this report). Hydrodynamics are an integral part of the design of this robot, as the impulse force produced by the combustible element of our design is the primary method of forward propulsion for our robot. With the 3 BCD design, the robot still maintains the same amount of orientation control as the previous 4 BCD design. Inflating the front BCD will allow the robot to tilt up, while inflating one of the rear BCDs will enable the robot to angle to the side. Thus, with only 3 BCDs, our design achieves two-axis rotation, while forward propulsion is achieved using impulse force induced by combustion. These three BCDs can easily be attached to the pill using M3 x 0.5 x 18 mm screws, as seen in Figure 32 below. See Figure 32 below for the CAD renders and the physical prototype of the entire pill with all the BCDs attached, the combustion chamber permanently affixed, and the lid design finalized.

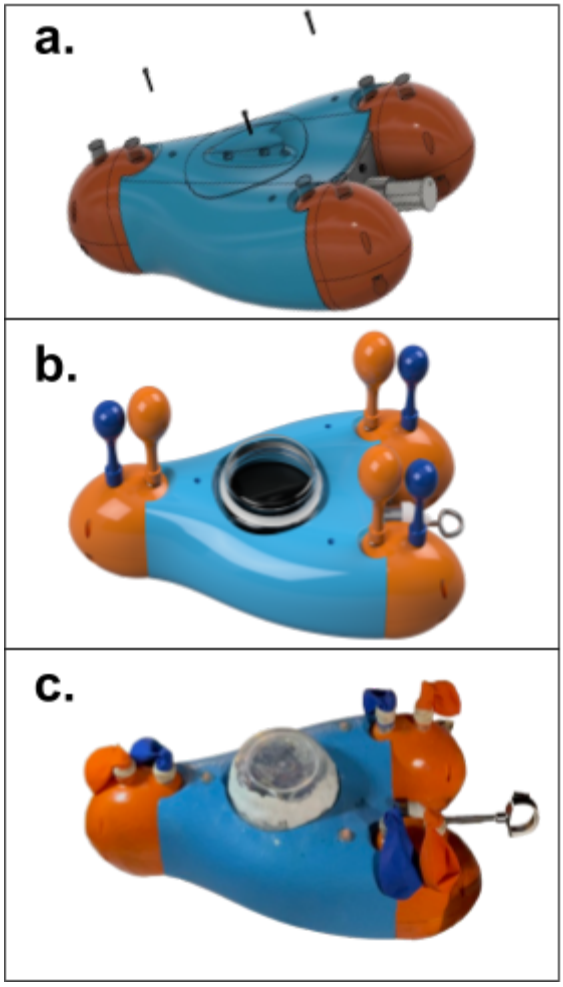

Figure 32: a. Preliminary CAD render of pill with BCDs with old lid design and the M3 screws used to attach the BCDs to the pill. b. Finalized CAD render of pill with BCDs attached, balloons, final lid design, and new combustion chamber. c. A physical prototype of the entire pill, all BCDs, and the combustion chamber are attached.

Waterproofing is an integral part of the design for this robot. In order to ensure that the electronic components and combustion system held within the robot are not damaged or disturbed, it was critical to design the pill such that it was 100% waterproof. First, the pill was designed in CAD and 3D-printed using PLA at 100% infill. Using 100% infill was not only necessary to help reduce cracks and prevent water from permeating through the surface of the robot, but it was also needed to increase the density and mass of the robot in order to achieve neutral buoyancy. If neutral buoyancy were not achieved, the robot would just float to the surface of the water uncontrollably. 3D-printing with 100% infill was also necessary to ensure the robustness and strength of the robot because it needed to withstand the force of the combustion without catastrophic mechanical failures, such as breaking or cracking. After the pill was printed, a number of post-processing steps were taken to ensure complete waterproofness.

Several coats of material were applied to both the outer and inner surfaces of the pill to prevent water from permeating through. Before each coat was applied, the previous one was completely dried and cured. First, an initial brush coating of Smooth-On XTC-3D epoxy was applied to the entire outer surface of the robot. Smooth-On XTC-3D has a set time of 10 minutes and a full cure time of around 4 hours. Then, a coat of Flex Seal spray liquid rubber sealant coating was applied to the outer surface of the robot. This Flex Seal Spray has a set time of around 2-3 hours and a full cure time of 24-48 hours. Then, two layers of J-B Weld quick-setting steel-reinforced epoxy were applied to the outer surface. J-B Weld steel reinforced epoxy has a set time of 6 minutes and a full cure time of 4-6 hours. Then, two coats of Rust-Oleum blue spray paint were applied to the outer surface. Rust-Oleum spray paint has a set time of 20 minutes and a full cure time of around 24 hours. These are all of the post-processing layers that were applied to the outside of the pill to achieve a water-tight surface. The different stages of these external layers can be seen in Figure 33 below.

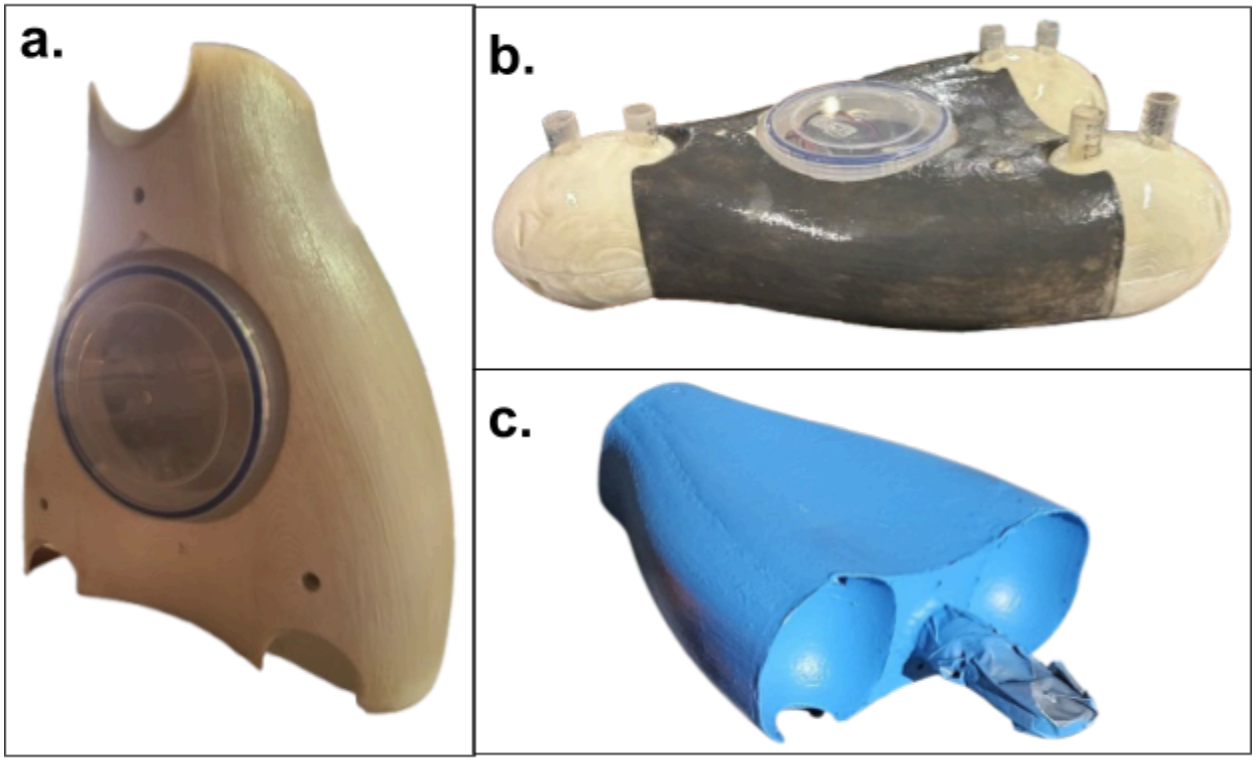

Figure 33: a. Pill with an outer coating of Flex Seal rubber spray. b. Pill with two coatings of J-B Weld steel reinforced epoxy and BCDs attached. c. The final pill, with two coatings of Rust-Oleum blue spray paint and a combustion chamber, is inserted into the back.

The inner surface of the pill also underwent post-processing procedures. First, the entire inner surface was coated with a thick layer of J-B Weld ClearWeld Quick Setting Epoxy. This epoxy has a set time of 5 minutes and a cure time of around 1 hour. Specific areas on the inner surface of the pill that were deemed as risky, possible points of leakage, were reinforced with J-B Weld WaterWeld Specially Formulated Epoxy Putty. This putty dries to a tough texture when fully cured and has a set time of 25 minutes and a full cure time of 1 hour. The wire holes

at each corner of the pill, where the wires that attach from the Arduino within the pill to the BCDs, also needed to be water-tight. These wire holes were sealed with layers of J-B Weld clear epoxy, cyanoacrylate super glue, and several layers of J-B Weld WaterWeld putty over top of all of those materials. After several waterproof testing trials, these methods achieved a 100% water-tight seal in the pill.

The lid of the pill also underwent several design iterations. The initial lid design, shown in Figure 33a, was initially designed to optimize hydrodynamics (as seen in the fin); however, it was not effective at waterproofing. This lid design utilized a radial O-Ring as its seal; however, this prevented it from fitting correctly into the pill. Therefore, a new lid, shown in Figures 33b and 33c, was created to maximize waterproofing at the expense of hydrodynamics. This lid design utilized the screw-on top of a Tupperware container, which already had an optimal O-ring seal built in. The Tupperware that was used is the LOCK & LOCK Easy Essentials Twist Food Storage container. This is the same container that was used as the previous team's (BAYMAX) BCD container. The top of this container was cut off and implemented into the pill. The male part of the lid was held in place using tack welds of cyanoacrylate super glue and permanently affixed to the opening in the pill using a copious amount of J-B Weld clear epoxy and J-B Weld WaterWeld putty. To ensure no water seeped through the threads, a fresh layer of Teflon was used every time the lid was removed.

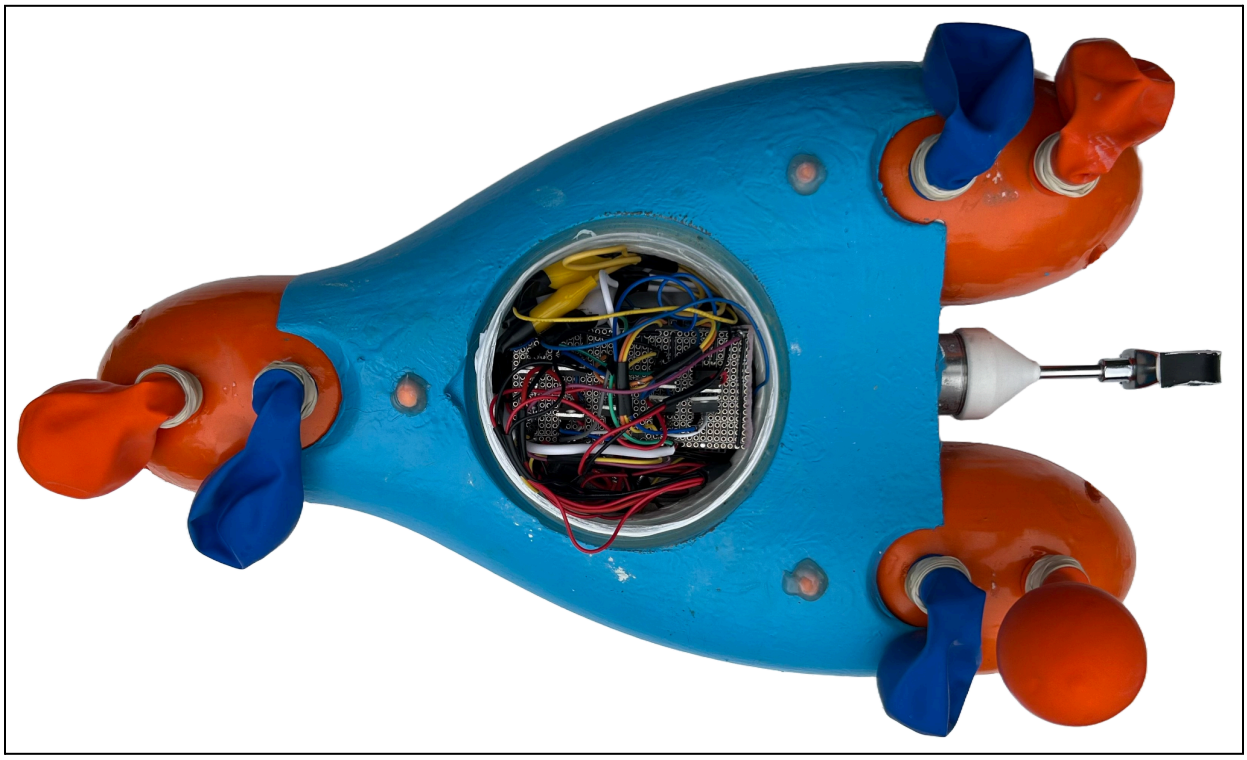

Figure 34: Top view of the entire robot with the wild removed and wiring exposed.

The combustion chamber was inserted into a pre-placed hole in the back of the pill. This chamber was secured Weld WaterWeld putty for both strength and waterproof effectiveness.

The initial design incorporated a metal plate that would ensure the combustion chamber of the pill. However, it was determined that for the purposes of simplicity and effective waterproofing, the use of epoxy putty was sufficient for mounting the chamber to the pill. In order to prevent the combustion chamber from launching into the pill post combustion, a separate piece, referred to as the “tombstone," was 3D-printed and mounted into the interior of the robot to prevent movement of the combustion chamber. The interior of the pill was also optimized to ensure that all the electronic components, the spark plug, and the ignition system could fit. A 9V battery holder was implemented into the design to hold the power source for the Arduino, and extra space was carved out of the inside to include room for the power banks that were used to power the electrolyzers. Despite these efforts, it was still tough to fit all of these components inside the pill, so the lid was adjusted and its height was increased to fit everything. The pill with all BCDs attached and electronics and combustion chamber inserted can be seen in the top view of the robot shown in Figure 34 above.

The BCD inserts in the pill were designed for ease of access and modularity. The BCDs are all attached to the pill via an M3 x 0.5 x 18 mm screw which can be accessed through holes on the top of the pill as shown in Figure 33a. Each BCD is attached and held in place using only one of these screws. Each BCD insert is also designed with extra space carved into the pill to accommodate wire slack for the wires that connect between the BCDs and the pill. Due to the fact that the 3D-print for the pill was done using 100% infill, printing warpage was a significant issue that we ran into. Specifically, when the print was done, the entire front half of the pill had detached from the hot plate and thus warped upward by a maximum of around 1 cm. This warpage prevented the front BCD from properly fitting into the pill. Reprinting the pill was not an option due to the expense and amount of PLA it takes, and the significant amount of time it would take to print such a large part with 100% infill. As such, a new BCD shell needed to be designed for the front of the robot. A LIDAR scan was used to scan the warped front section of the pill, and this scan was used to redesign a new BCD shell for the front BCD in CAD. Once this was done, the new BCD fit correctly into the warped front insert on the pill.

Neutral buoyancy is an essential component of this robot. If the density of the entire robot is less than that of water, 1000 kg/m^3, it will float to the top uncontrollably. If its density is the same or greater than that of water, then the balloons can be inflated to control their depth in water and orientation. Thus, to achieve neutral buoyancy of the entire robot in water, we needed the robot to have a density near that of water or at least greater. Once the whole robot prototype was put together, its total mass was 4864 g, including the pill, the BCDs, the combustion chamber, and all electronic components. Based on the CAD model in Fusion, the robot’s volume was 0.005203 m^3. This resulted in a calculated value of 934.8 kg/m^3 for the density of the robot. As such, artificial weights in the amount of at least 340 g needed to be added to the robot to achieve neutral buoyancy. A 1-inch-thick solid steel bar was cut into chunks, which were placed inside the pill to increase its density to 1000 kg/m^3 and ensure neutral buoyancy.

Results

Our final results consist of the complete effectiveness of the robot during the fully integrated underwater test. The assembled robot performed adequately and as designed. We observed absolutely no leaking even after 3 hours of testing with the robot completely submerged. The robot has achieved 4 DOF movement with rotation roll and pitch as well as linear motion about the x axis and the z axis. Additionally, the design is capable of reliable electrolysis-driven combustion.

The entire integrated robot test procedure was documented and recorded for reference and analysis. The Tracker software was used to analyze the recording of the test and determine the combustion capabilities of the design including distance traveled, linear acceleration, and thrust force. An image of the analysis is captured below.

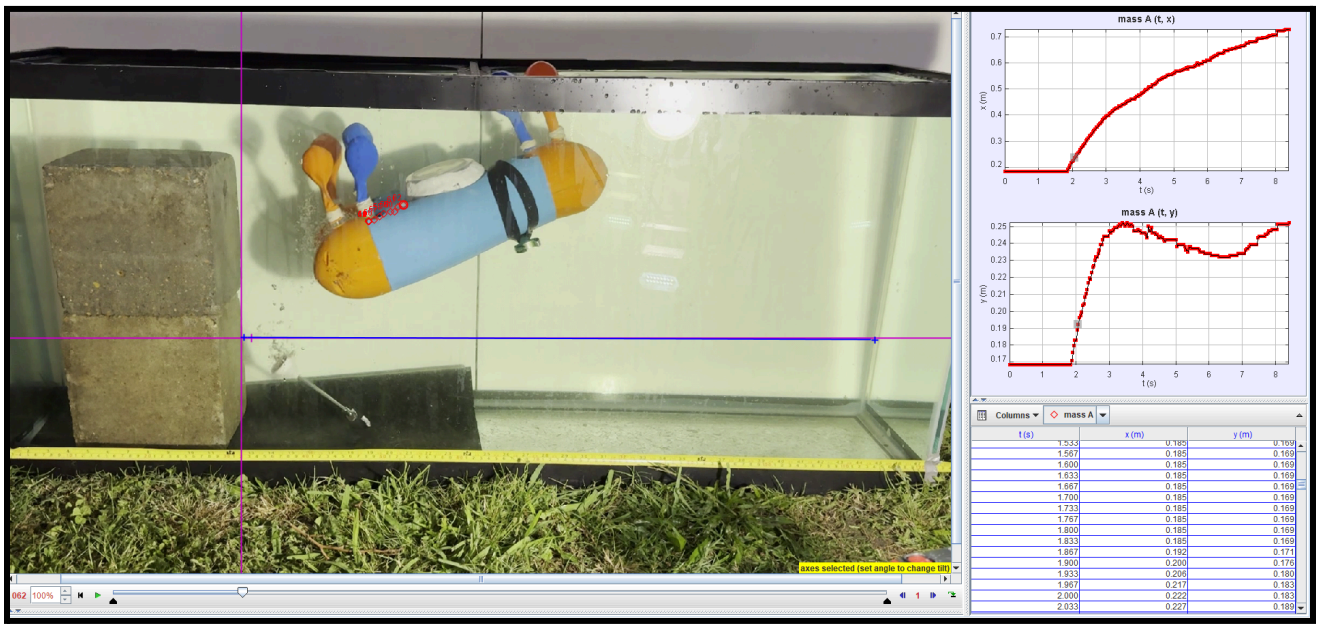

Figure 35: Integrated Test - Tracker Analysis

It was estimated that the robot achieved a peak acceleration of 3 m/s^2. Given that the robot weighs 5kg, it can be calculated that the robot achieved a forward force of 15 N. This reflects the force captured from the linear combustion tests since those tests achieved a force of 21.45 N. The drop in forward force is due to the drag from the body of water. Overall, the software captured reasonable data since there is little noise, and the bobbing motion was captured well by the change in position along the vertical axis.

A Brief History of the Project

Our project is a continuation of previous underwater robots that Professor Ghorbel's Robotics and Intelligent Systems Lab (RiSyS) has sponsored as a senior design project. Last year's lab-sponsored project, Team Baymax, introduced the novel concept of using reversible fuel cells as buoyancy control devices (BCDs). In their robot, the reversible fuel cells would operate as an electrolyzer to use electricity to convert distilled water into H2 and O2 gas that would inflate four pairs of balloons. Their increasing volume increases the buoyancy of the entire robot, causing it to rise underwater. When operating in fuel cell mode, their robot would theoretically convert the gases in the balloons back into water and energy, thus deflating the balloons. The decreasing volume lowers the buoyancy of the entire robot, causing it to sink underwater. However, their robot was not entirely soft, since they used motors and propellers. The initial goal for our robot, MUDKIP, was to continue improving on the BCDs and make them smooth and possibly untethered. Most importantly, we were tasked with using a combustion reaction by igniting the H2 and O2 mixture to produce jumping action, similar to that of a mudskipper.

Initially, we went through many ideas, including building our own custom reversible fuel cell to maximize production both ways. We eventually veered off this path after our professor advisors told us to, since it would be an entire project in itself to design and make our own reversible fuel cells. So instead, we bought commercial off-the-shelf reversible fuel cells from the FuelCellStore. We ran some tests with it, but found that it never worked well as a fuel cell since there would be water clogging the pipes and membranes, preventing the lower-pressure input gases from entering the fuel cell. We never found a viable solution to this that would fit the size constraints of our robot. Furthermore, the oxygen output was never up to our expectations because of flimsy rubber flaps in the reversible fuel cell, which were meant to take in outside air (a mixture of nitrogen, oxygen, and more) when operating as a fuel cell. Instead, the oxygen we produced in electrolyzer mode escaped through these hatches. With all these problems, we ended up buying electrolyzers instead, which meant buoyancy control could only work to increase, not decrease, the buoyancy. Because complete buoyancy control was not our main objective and could be demonstrated under different robot size constraints, it was acceptable to utilize just electrolyzers for our other objectives.

Using just electrolyzers to produce oxygen and hydrogen gas was sufficient for our two objectives of swimming and jumping. At first, we wanted to be able to swim in the water using a silicone molded fish tail that sways when its interior is alternately filled with gases. We built several prototypes for this and actually demonstrated it working using a high-pressure bicycle pump. Yet this is also the reason why we ended up cancelling this objective. After consulting our professor advisors at the end of the fall semester, we agreed that it was infeasible to operate the fish tail design under our robot constraints due to the sheer amount of gases and pressure needed to inflate and properly move the tail. Our robot was too small and did not have the space to store electrolyzers that produce large volumes of gases at sufficiently high pressures. Our revised goals for the spring semester were to have a soft, tetherless robot that used BCDs

to only inflate balloons for increasing buoyancy and have a combustion chamber that facilitates combustion reaction for forward propulsion. The net result would be adjusting the header angle of our robot to have the front side higher in elevation than the back side, and utilizing the combustion reaction to thrust the robot up at an angle and hopefully out of water, as if it were jumping like a mudskipper.

Our spring semester was spent redesigning the chassis of the robot, called the pill, along with the three detachable BCDs. We also spent tens of hours waterproofing the robot, trying everything from printing at 100% infill to prevent leaks due to porous structures, glazing it with epoxy to form a barrier, teflon tape in our twistable pill cover, and pairs of o-rings in the BCDs to keep water out. We also did considerable research and development into constructing a durable yet large combustion chamber that could consistently operate without concern for damaging the rest of the robot. Prototypes of this were made in the fall semester, and we conducted successful tests with it, not in water but using linear rails, thus collecting velocity and acceleration data. The spring semester was all about compacting the design, making it resemble a syringe that started as a vacuum and gradually filled with a pure mixture of H2 and O2 gas without leaks, enabling us to have powerful, robust, and reliable propulsion in water. The electrical circuit also changed dramatically. In the fall semester, we had a 30-foot-long wire test setup that detonated the gases using a pushable grill ignitor. This was too bulky and required applied pressure to work, which meant it was only good enough for prototyping. Later, we tried using an ignition coil and spark plug setup meant for RC cars since it has the same final result of amplifying input voltages by thousands of times. The ignition coil failed because of insufficient input charge (current) despite having the proper voltage. Therefore, our final ignition circuit utilized a high-voltage transformer that amplified our input of 5V and a small current to kilovolts, which went to the spark plug. This was able to produce sparks and ignite our gases under conditions similar to a car's combustion chamber, though it was not able to do it consistently since the spark plugs warped a few times during actual use. We also powered the electrolyzers using high ampere-hour battery banks, which enabled gas production at the advertised rates of 20 ml H2/min and 10 ml O2/min. Without this fast production, our BCDs and combustion chambers would not have worked as well as they did, demonstrated by the lackluster performance when using low-charge 9V batteries. To control the ignition and electrolyzer circuits, we devised an electronic circuit utilizing transistors for current flow control, a flyback diode for protection against inductive emf flowback, and other passive components for design stability. We soldered all connections onto a perf board and taped the wire ends to our Arduino, then carefully jammed it inside the waterproofed pill of our robot. To control all the BCDs and ignition circuit, we wrote software that enabled the usage of the Arduino's WiFi capabilities, letting us send signals to remotely turn components on and off at a safe distance. This is what makes our soft robot a tetherless design, achieving a significant milestone for the semester.

In the end, we were able to show successful BCD operation underwater, combustion resulting in propulsion underwater, and both combined in the same test. All this is on video, which will be shown during our presentation. We had to learn many new skills along the way, learn how to work around each other's schedules, and individually take initiative and lead each

other when the situation called for it. This year-long project definitely prepared us to tackle similar and even more challenging scenarios in industry and academia.

Future Work

1. Power regeneration from the reverse electrolysis process:
   The current fuel cell technology features an efficiency trade-off between the forward and reverse electrolysis processes. Currently, optimal (forward) electrolyzers and (reverse) fuel cells feature different membrane compositions. An optimal forward electrolyzer cannot operate in reverse, as the membrane will be soaked and cease to function. In the interest of efficiency and due to our inability to invent new fuel cell membrane technology, we designed a robot that could control a fuel cell in both directions but only operated in forward mode. Implementing reverse mode, while not difficult, opens up the idea of storing the electricity produced in that reaction as energy, which would further improve the robot's energy efficiency.
2. Designing a system capable of generating internal pressure in the combustion chamber:
   Currently, our combustion chamber is single-use and relies on a plunger that moves outward as the chamber is filled with gas. Designing a system that can generate internal pressure allows the combustion chamber to hold more gas for a stronger explosion, and a reusable such mechanism will enable repeatability in the explosblastng the robot viable to send on missions.
3. Autonomous control algorithms and sensors:
   Control was not possible with the current robot, as feedback-based control requires the ability for fuel cells to operate in reverse. Implementing basic PI/D controls or more advanced sensor-based controls will allow the robot to better make use of the buoyancy control capabilities. The sensors would also be able to collect real-time environmental data during exploration.
4. Improve the strength of the wireless communication:
   Currently, we are testing 2.4GHz wifi as a proof of concept, but this signal does not travel far enough underwater for practical applications.

Conclusion and lessons learned.

We ended up meeting the updated requirements set out by Dr. Ghorbel for the project. It took a sizable amount of time during the Fall semester to narrow down what the criteria should be, as a "soft robot that can jump and glide" can take many forms, some of which were definitely beyond the scope of a year's work. Dr. Ghorbel expressed satisfaction with our results during our meetings. While our prototype is currently not ready for commercialization, it succeeded as a proof-of-concept for Dr. Ghorbel and Dr. Schaefer's research efforts. Further efforts towards the action items in the "future works" section will definitely make the robot a viable option for aquatic environment survey applications – there are directions that are both more R&D-based and application-based in these, both of which could make for interesting future projects.

With regards to the lessons we learned, the biggest one is the difficulty to predict how things will turn out. When we first heard our advisors tell us they wanted to build a soft-actuated, tetherless, underwater vehicle that utilizes the combustion reaction of H2 and O2 gas to jump out of water, it was frankly a lot to take in. We had no idea where to begin, as there are few examples of similar robots out there. We were basically tasked to create something actually new. The first few weeks and months were just spent brainstorming any and all ideas, each of which was quickly shot down as too ambitious or challenging to build due to an abundance of potential failure points. It was not until we grounded ourselves by building tangible prototypes that tested each of the processes we wanted to achieve that we felt more assured and saw real progress being made. The combustion reaction test rig showed us what our final chamber needed to look like. The limitations with ignition informed us what the electronics needed, like at the end, in order to consistently ignite and also operate the BCDs. Tons of test 3D print components guided our BCD development over the iterations. We also ended up sufficiently narrowing the scope of our project at the end of the fall semester, which made it more realistic in the time frame we had left. Luckily, we were able to get a working prototype by showcasing, but barely so. Since it is so difficult to predict how things will turn out, even with a solid plan and Gantt chart, it is essential to get scared of the big picture and just start prototyping the core mechanisms. Rapid prototyping will definitely show us something about failure and success. If we had started the rapid prototyping weeks earlier, we would have a more refined project by the end of the spring semester.

In the end, we did manage to downscale and improve upon last year's team's functionalities, in addition to proving the "entirely soft actuated underwater robot" and "electrolysis-based explosion as movement" concepts. Our tangible impacts are listed in detail below.

Impacts:

- Our robot is entirely soft actuated and buoyancy-based, meaning it does not constantly consume power to stay at a constant depth.
- Our robot is self-contained: wirelessly and tetherlessly controlled, which improves the range of areas to which it can be deployed.
- Our robot is cheap and energy-efficient: in a world where underwater robots require a large battery or power outlet to function and cost thousands of dollars, our robot is powered with two phone-charging power banks and a 9V battery and costs $500.
- We demonstrated the viability of electrolysis-based buoyancy control and propulsion in underwater robots, especially in a considerably downsized version compared to last year's.

Appendices

A1: Assembly Instruction Manual

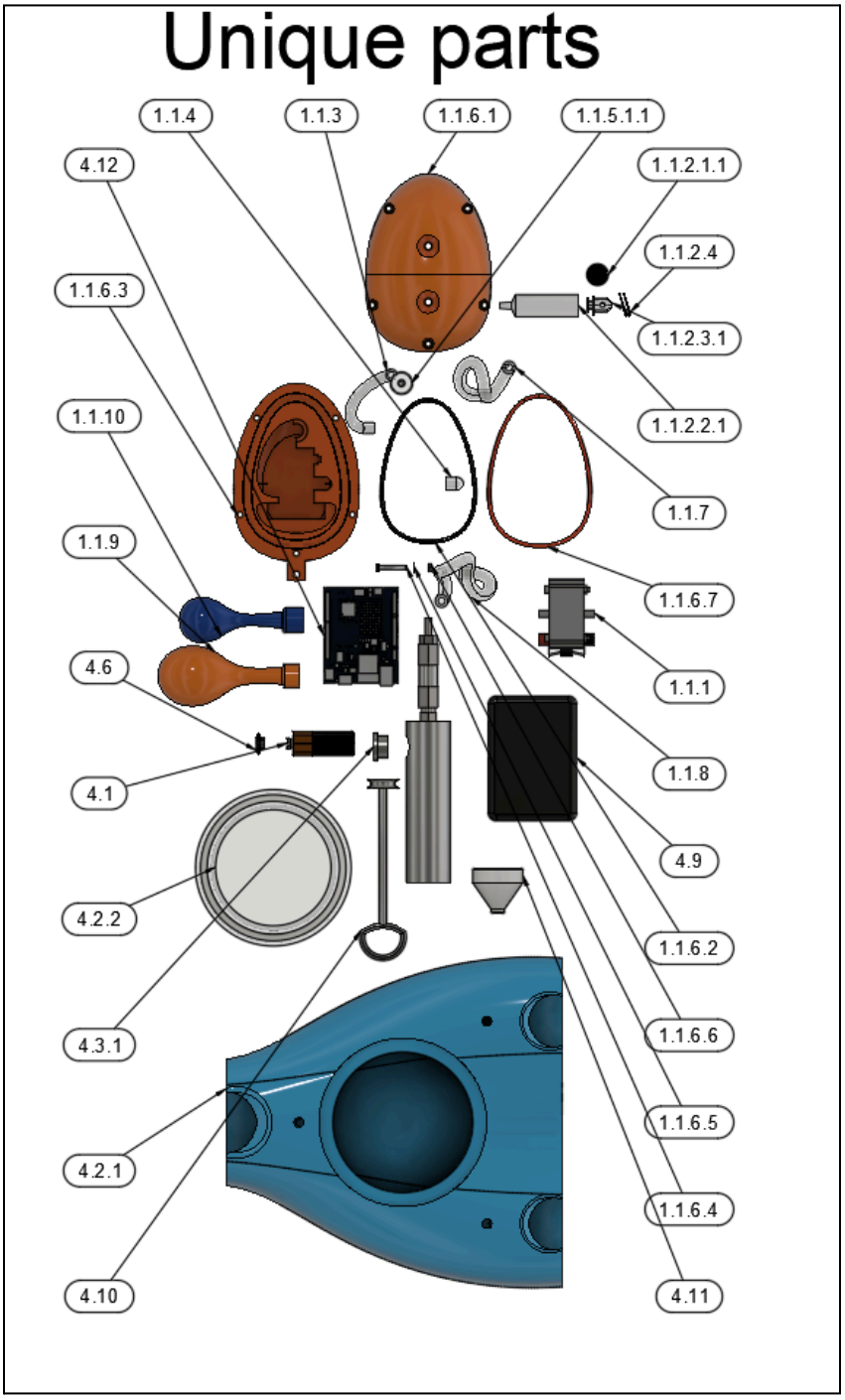

BCD Steps

Step 1: Epoxy and paint

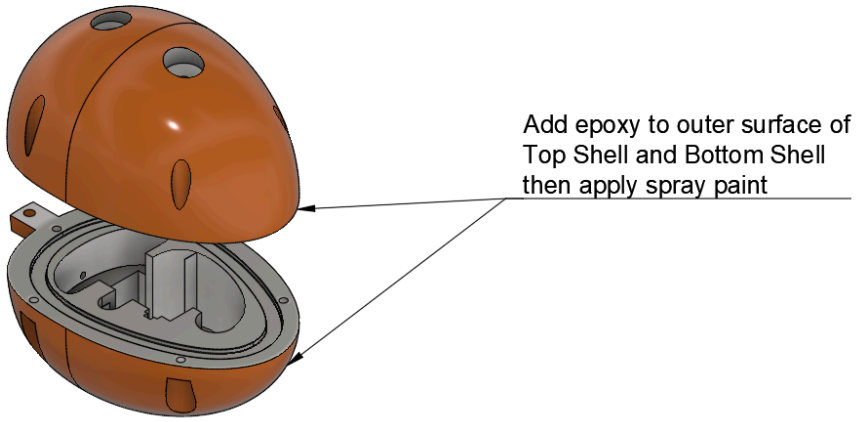

Step 2: Insert Wires

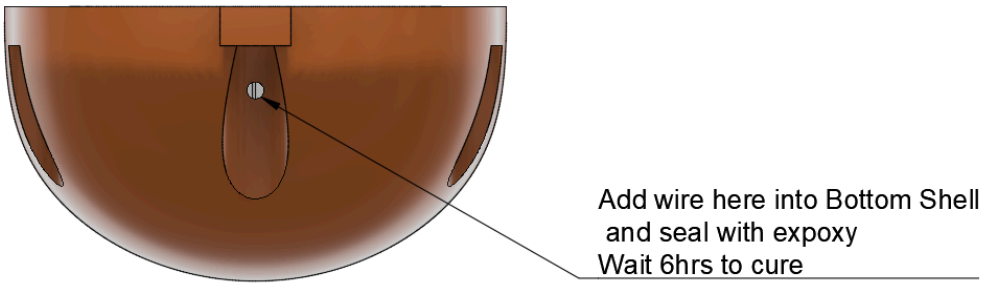

Step 3: Apply Tubing

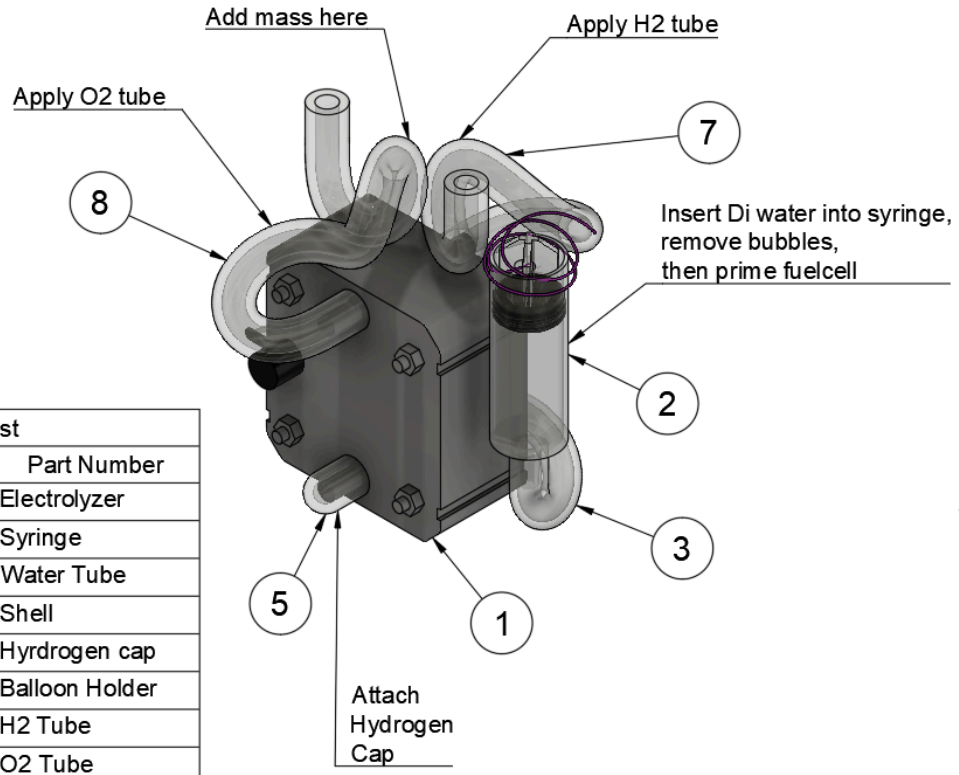

Parts List		
Item	Qty	Part Number
1	1	Electrolyzer
2	1	Syringe
3	1	Water Tube
4	1	Shell
5	1	Hyrdrogen cap
6	2	Balloon Holder
7	1	H2 Tube
8	1	O2 Tube
9	1	H2 Balloon
10	1	O2 Balloon

Step 4: Place Internals in the Shell

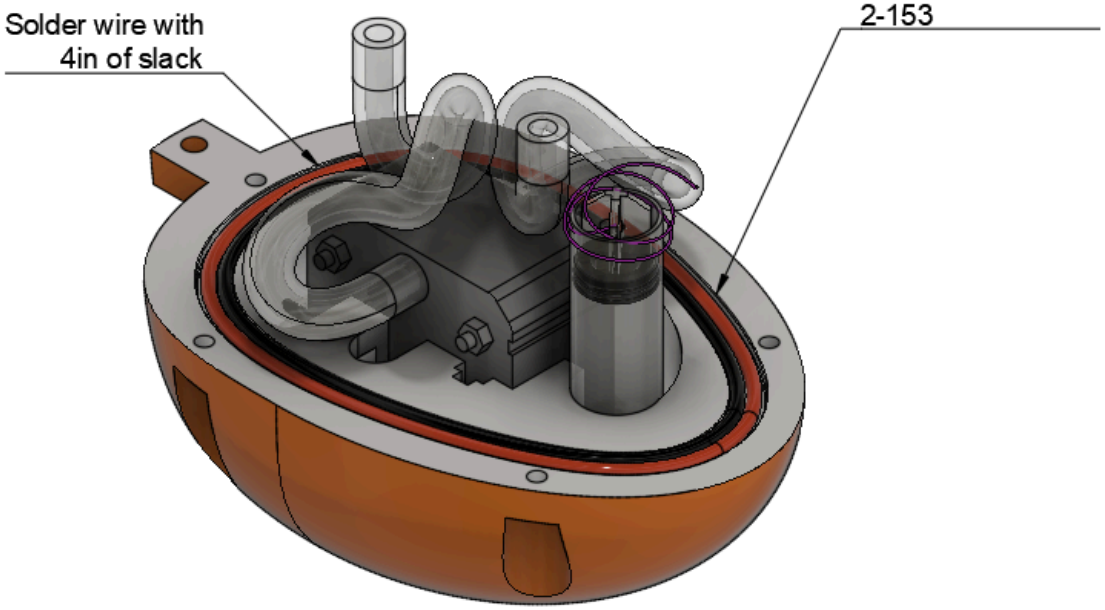

Step 5: Attach Balloon Holders to Top Shell

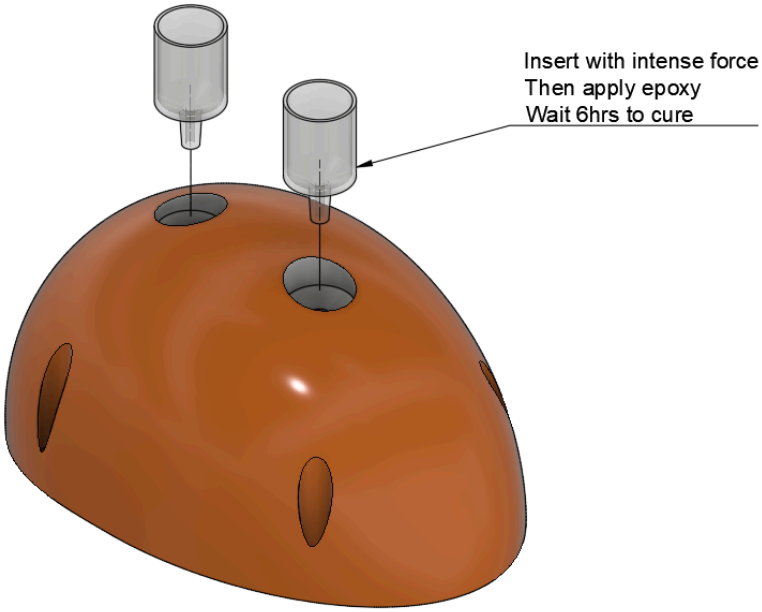

Step 6: Attach tubes to Balloon Holders

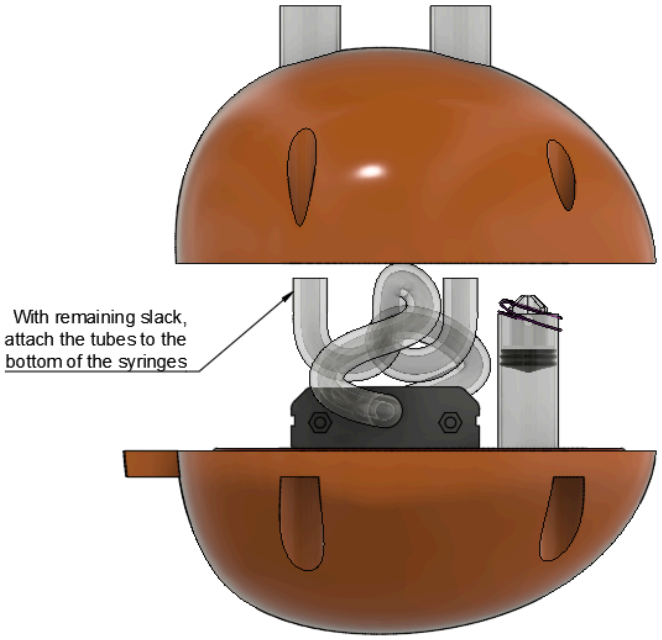

Step 7: Prepare Screwing

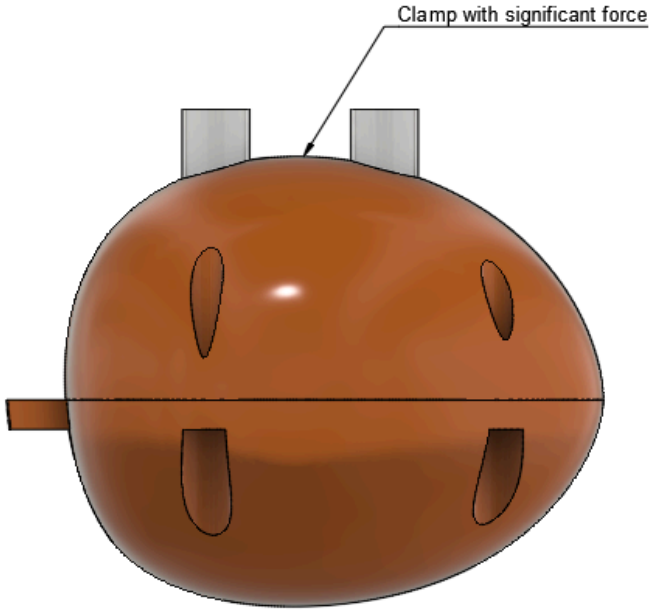

Step 8: Screw Together

Parts List		
Item	Qty	Part Number
1	1	Electrolyzer
2	1	Syringe
2.1	1	Barrel
2.1.1	1	Barrel_1.step
2.2	1	Gasket
2.2.1	1	Gasket_1.step
2.3	1	Plunger
2.3.1	1	Plunger_1.step
2.4	1	String
3	1	Water Tube
4	1	Shell
4.1	1	Top Shell
4.2	1	Bottom Shell
4.3	1	O'Ring 2-152
4.4	5	---
4.5	5	98269A420_Black-Oxide 18-8 Stainless Steel Washer
4.6	5	90448A110_Metric 18-8 Stainless Steel Sealing Hex Nut
4.7	1	O'Ring 2-153
5	1	Hyrdrogen cap
6	2	Balloon Holder
6.1	1	Barrel
6.1.1	1	Barrel_1.step
7	1	H2 Tube
8	1	O2 Tube
9	1	H2 Balloon
10	1	O2 Balloon

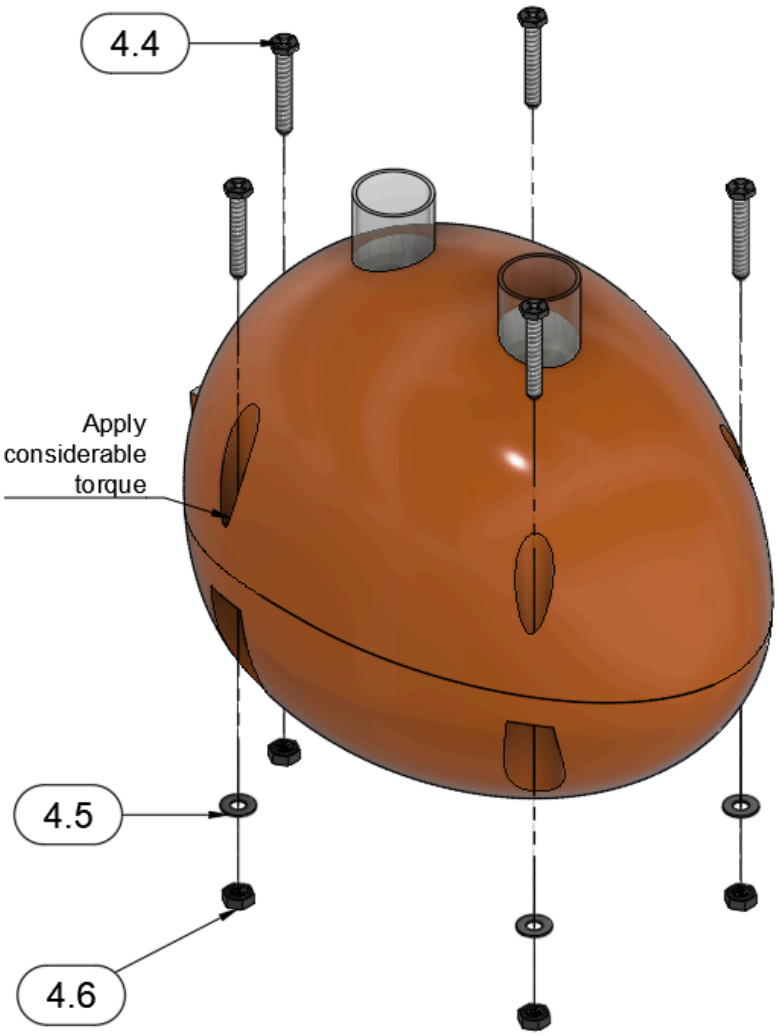

Step 9: Attach Balloons
Then repeat these nine steps to create three BCDs

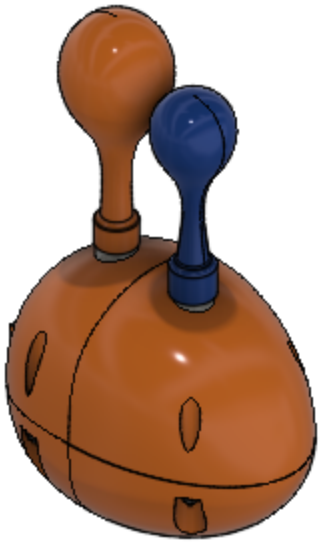

Pill Steps

Step 1: Apply Outer sealants

1. Flex seal (24hr cure time)
2. XTC-3D (6hr cure time)
3. 1 coat of steel reinforced epoxy (6hr cure time)
4. Apply second coat of steel reinforced epoxy

Do not apply to interactive faces where labeled

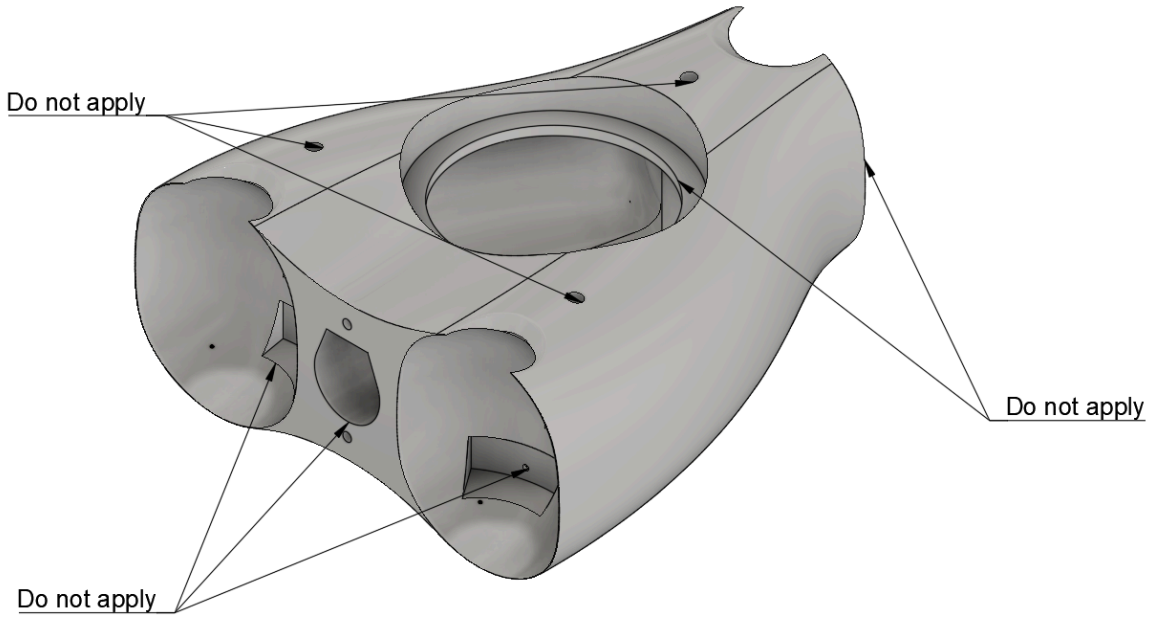

Step 2: Insert Combustion Chamber

- Insert combustion chamber then rotate 90deg
- Apply significant amounts of JB Underwater Weld to the surface the chamber contacts with the Pill
- Spray paint once completed

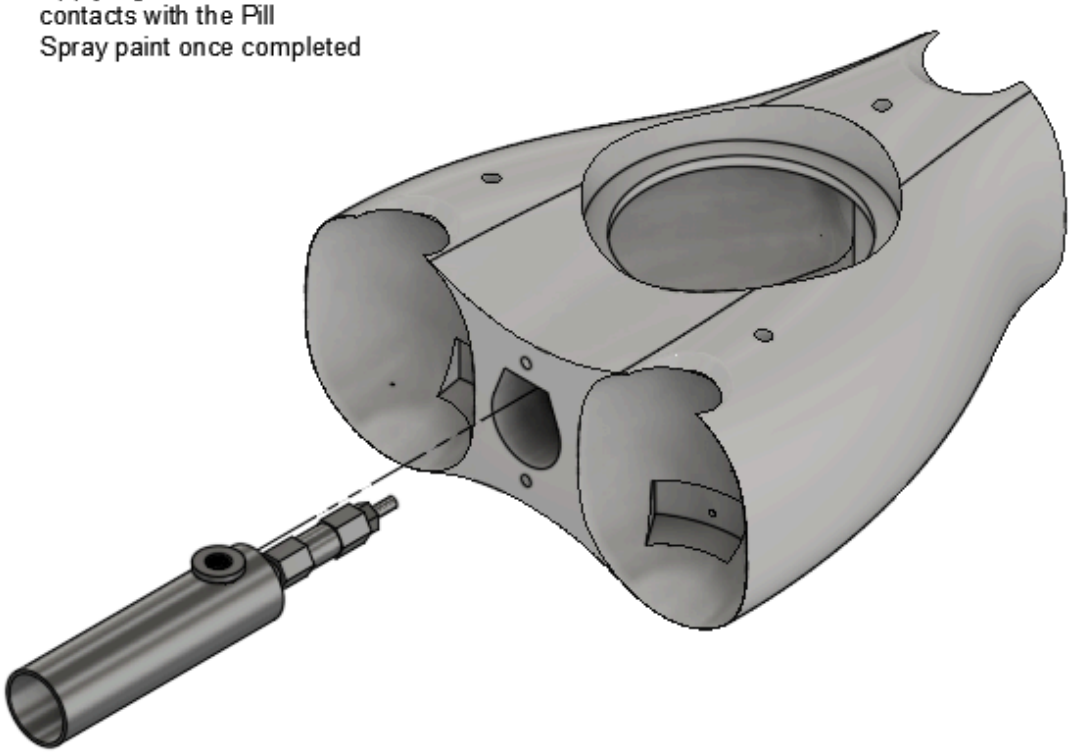

Step 3: Insert BCD into PIII

- insert wire through wire hole in the PIII, and seal with epoxy and multiple layers of JB Underwater Weld
- Repeat this for each BCD

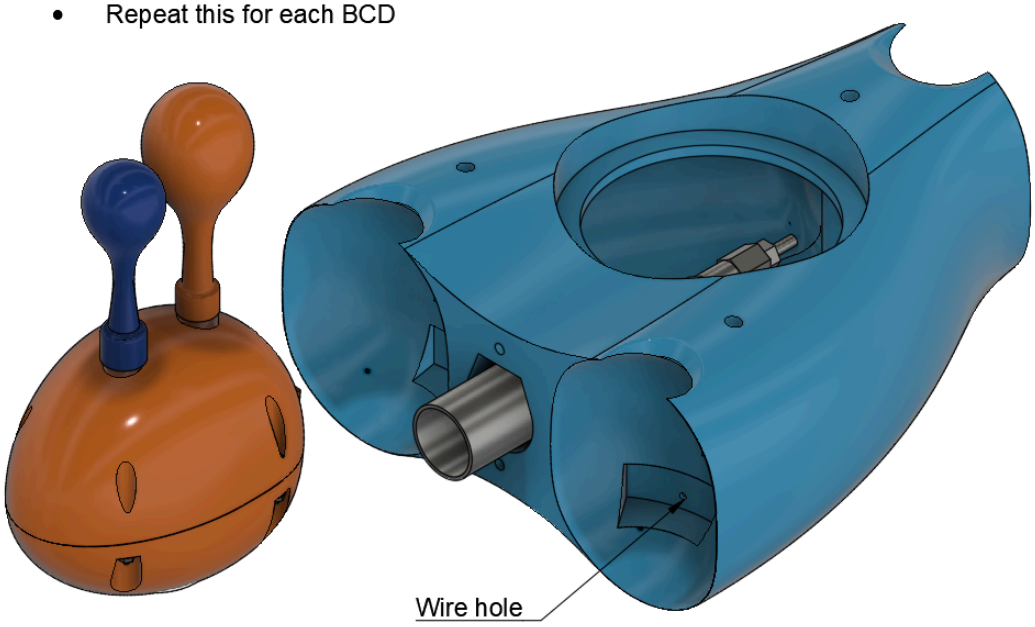

Step 4: Attach Tupperware© Lid

- Apply the cut portion of the Tupperware base to the flat area of the Pill.
- To fasten it, center it, then apply "tack-welds" of super glue.O
- Once hardended, apply significant epoxy in the gap between the Lid and the Pill.

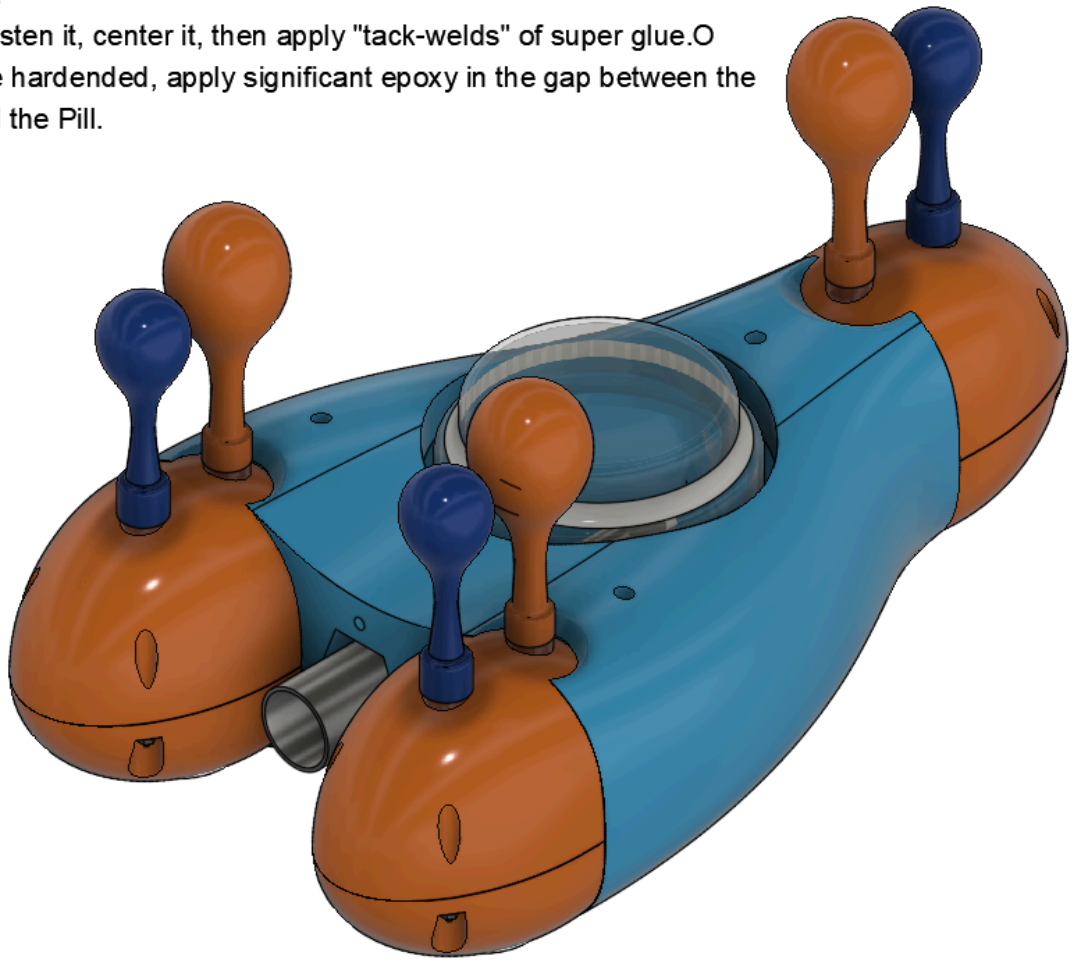

Step 5: Add Electronics and Finalize Combustion Chamber

Add the following inside the Pill to complete the robot

- Electrolyzer
- Arduino R4
- Two batteries
- Blast Cap
- Plunger
- 9V battery

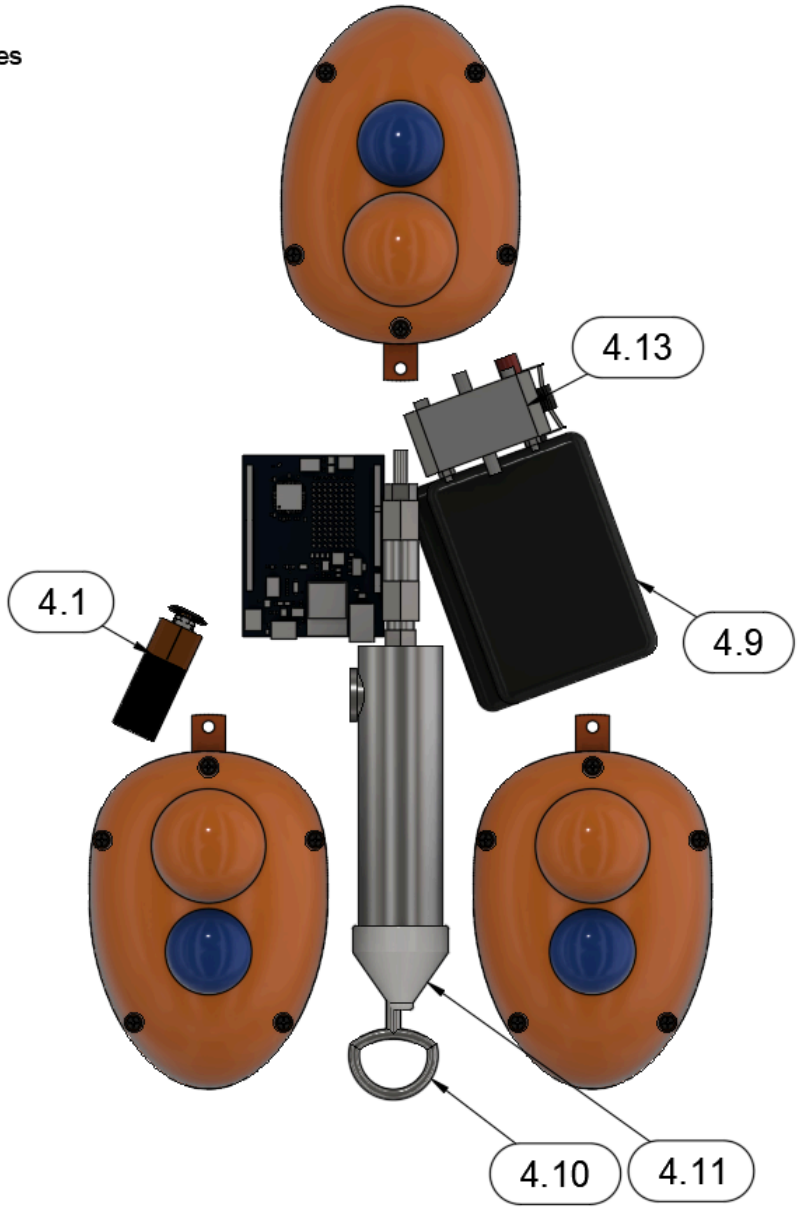

A2: Bill of Materials

Table A2: BOM				
Item	**Qty**	**Part Number**	**Unit Price**	Total Price
1	1	BCD Front		$0.00
1.1	1	BCD - Base v165		$0.00
1.1.1	1	Electrolyzer v3	$110.00	$110.00
1.1.2	1	Syringe v16	$0.18	$0.18
1.1.2.1	1	2-152	$1.27	$1.27
1.1.2.1.1	1	Gasket_1.step		$0.00
1.1.2.2	1	Barrel		$0.00
1.1.2.2.1	1	Barrel_1.step		$0.00
1.1.2.3	1	Plunger		$0.00
1.1.2.3.1	1	Plunger_1.step		$0.00
1.1.2.4	1	String	$0.20	$0.20
1.1.3	1	Water Tube	$0.40	$0.40
1.1.4	1	Hydrogen cap	$0.03	$0.03
1.1.5	2	Balloon Holder v3	$0.18	$0.36
1.1.6	1	Shell		$0.00
1.1.6.1	1	Top Shell		$0.00
1.1.6.2	1	O'Ring 2-152	$1.27	$1.27
1.1.6.3	1	Bottom Shell		$0.00
1.1.6.5	5	98269A420_Black-Oxide 18-8 Stainless Steel Washer	$0.02	$0.12
1.1.6.6	5	90448A110_Metric 18-8 Stainless Steel Sealing Hex Nut	$6.05	$30.25
1.1.6.7	1	O'Ring 2-153	$6.37	$6.37
1.1.7	1	H2 Tube	$0.40	$0.40

1.1.8	1	O2 Tube	$0.40	$0.40
1.1.9	1	H2 Balloon	$0.20	$0.20
1.1.10	1	O2 Balloon	$0.20	$0.20
2	1	BCD Right		$0.00
2.1	1	BCD - Base v165		$0.00
2.1.1	1	Electrolyzer v3	$110.00	$110.00
2.1.2	1	Syringe v16	$0.18	$0.18
2.1.2.1	1	2-152	$1.27	$1.27
2.1.2.2	1	Plunger	$5.00	$5.00
2.1.2.2.1	1	Plunger_1.step		$0.00
2.1.2.4	1	String	$0.20	$0.20
2.1.3	1	Water Tube	$0.05	$0.05
2.1.4	1	Hydrogen cap	$0.03	$0.03
2.1.5	2	Balloon Holder v3	$0.18	$0.36
2.1.6	1	H2 Tube	$0.40	$0.40
2.1.7	1	O2 Tube	$0.40	$0.40
2.1.8	1	Shell		$0.00
2.1.8.1	1	Top Shell	$2.20	$2.20
2.1.8.2	1	O'Ring 2-152	$1.27	$1.27
2.1.8.3	1	Bottom Shell	$3.00	$3.00
2.1.8.4	5	----		$0.00
2.1.8.5	5	98269A420_Black-Oxide 18-8 Stainless Steel Washer	$0.30	$1.50
2.1.8.6	5	90448A110_Metric 18-8 Stainless Steel Sealing Hex Nut	$0.02	$0.12
2.1.8.7	1	O'Ring 2-153	$6.37	$6.37
2.1.9	1	H2 Balloon	$0.20	$0.20
2.1.10	1	O2 Balloon	$0.20	$0.20
3	1	BCD Left		$0.00

3.1	1	BCD - Base v165		$0.00
3.1.1	1	Electrolyzer v3	$110.00	$110.00
3.1.2	1	Syringe v16	$0.18	$0.18
3.1.2.1	1	2-152	$1.27	$1.27
3.1.2.4	1	String	$0.01	$0.01
3.1.3	1	Water Tube	$0.40	$0.40
3.1.4	1	Hydrogen cap	$0.03	$0.03
3.1.5	2	Balloon Holder	$0.18	$0.36
3.1.6	1	H2 Tube	$0.40	$0.40
3.1.7	1	O2 Tube	$0.40	$0.40
3.1.8	1	Shell		$0.00
3.1.8.1	1	Top Shell	$2.20	$2.20
3.1.8.2	1	O'Ring 2-152	$1.27	$1.27
3.1.8.3	1	Bottom Shell	$3.00	$3.00
3.1.8.4	5	----		$0.00
3.1.8.5	5	98269A420_Black-Oxide 18-8 Stainless Steel Washer	$0.02	$0.12
3.1.8.6	5	90448A110_Metric 18-8 Stainless Steel Sealing Hex Nut	$6.05	$30.25
3.1.8.7	1	O'Ring 2-153	$1.36	$1.36
3.1.9	1	H2 Balloon	$0.20	$0.20
3.1.10	1	O2 Balloon	$0.20	$0.20
4	1	Pill		$0.00
4.1	1	9V-battery	$2.75	$2.75
4.3	1	MetalChamber	$10.16	$10.16
4.3.1	1	Welding-socket-collar-M10x1-B	$10.00	$10.00
4.4	1	Syringe	$0.18	$0.18

4.4.2	1	2-152	$1.27	$1.27
4.4.4	1	String	$0.01	$0.01
4.6	1	9V Battery Clip Connector	$0.50	$0.50
4.7	3	92290A761_Super-Corrosion-Resistant 316 Stainless Steel Socket Head Screw	$0.28	$0.85
4.8	3	91828A211_18-8 Stainless Steel Hex Nut	$0.05	$0.14
4.9	2	Battery	$4.20	$8.40
4.1	1	Plunger	$2.40	$2.40
4.11	1	Blast_cap	$0.11	$0.11
4.12	1	UNO R4 WiFi_Simplify_3	$28.00	$28.00
4.13	1	Electrolyzer	$110.00	$110.00
				$610.83

References

[1] “Membrane Electrode Assemblies (MEA),” *www.fuelcellstore.com*. https://www.fuelcellstore.com/fuel-cell-components/membrane-electrode-assembly

[2] A. D. Marchese, C. D. Onal, and D. Rus, “Autonomous Soft Robotic Fish Capable of Escape Maneuvers Using Fluidic Elastomer Actuators,” *Soft Robotics*, vol. 1, no. 1, pp. 75–87, Mar. 2014, doi: https://doi.org/10.1089/soro.2013.0009.

[3] “Double Reversible Fuel Cell H2/O2/Air,” *Fuelcellstore.com*, 2024. https://www.fuelcellstore.com/fuel-cell-stacks/double-rfc-h2o2-air-r104 (accessed Dec. 18, 2024).

[4] Y. Chen *et al.*, “A biologically inspired, flapping-wing, hybrid aerial-aquatic microrobot,” *Science Robotics*, vol. 2, no. 11, Oct. 2017, doi: https://doi.org/10.1126/scirobotics.aao5619.

[5] Moran, M. J., & Shapiro, H. N. (2018). *Fundamentals of Engineering Thermodynamics*. Wiley.

[6] *Emergency procedures*. Environmental Health and Safety | Rice University. (n.d.). https://safety.rice.edu/emergency-procedures

[7] Kromschroeder. (n.d.-b). https://docuthek.kromschroeder.com/download.php?lang=de&doc=63792

[8] General Environmental, Health, and Safety (EHS) guidelines. (n.d.-a). https://www.ifc.org/content/dam/ifc/doc/2023/ifc-general-ehs-guidelines.pdf

[9] Santora, M. (2019, July 24). *Bearing Friction Basics: A Primer*. Bearing Tips. https://www.bearingtips.com/bearing-friction-basics-primer/

[10] Wikimedia Foundation. (2024, December 3). *Drag coefficient*. Wikipedia. https://en.wikipedia.org/wiki/Drag_coefficient

[1] “Membrane Electrode Assemblies (MEA),” *www.fuelcellstore.com*. https://www.fuelcellstore.com/fuel-cell-components/membrane-electrode-assembly
[2] A. D. Marchese, C. D. Onal, and D. Rus, “Autonomous Soft Robotic Fish Capable of Escape Maneuvers Using Fluidic Elastomer Actuators,” *Soft Robotics*, vol. 1, no. 1, pp. 75–87, Mar. 2014, doi: https://doi.org/10.1089/soro.2013.0009.
[3] “Double Reversible Fuel Cell H2/O2/Air,” *Fuelcellstore.com*, 2024. https://www.fuelcellstore.com/fuel-cell-stacks/double-rfc-h2o2-air-r104 (accessed Dec. 18, 2024).
[4] Y. Chen *et al.*, “A biologically inspired, flapping-wing, hybrid aerial-aquatic microrobot,” *Science Robotics*, vol. 2, no. 11, Oct. 2017, doi: https://doi.org/10.1126/scirobotics.aao5619.
[5] Moran, M. J., & Shapiro, H. N. (2018). *Fundamentals of Engineering Thermodynamics*. Wiley.

[6] *Emergency procedures*. Environmental Health and Safety | Rice University. (n.d.). https://safety.rice.edu/emergency-procedures
[7] Kromschroeder. (n.d.-b). https://docuthek.kromschroeder.com/download.php?lang=de&doc=63792
[8] General Environmental, Health, and Safety (EHS) guidelines. (n.d.-a). https://www.ifc.org/content/dam/ifc/doc/2023/ifc-general-ehs-guidelines.pdf
[9] Santora, M. (2019, July 24). *Bearing Friction Basics: A Primer*. Bearing Tips. https://www.bearingtips.com/bearing-friction-basics-primer/
[10] Wikimedia Foundation. (2024, December 3). *Drag coefficient*. Wikipedia. https://en.wikipedia.org/wiki/Drag_coefficient